Environmental Sciences Europe

RESEARCH

Open Access

The risk may not be limited to flooding: polluted flood sediments pose a human health threat to the unaware public

Alexandra Weber[1*], Stefanie Wolf[2], Nadine Becker[3], Leonie Märker-Neuhaus[2], Piero Bellanova[4], Catrina Brüll[2], Henner Hollert[3,5,6], Elena-Maria Klopries[2], Holger Schüttrumpf[2] and Frank Lehmkuhl[1]

Abstract

Background Because of global climate change, extreme flood events are expected to increase in quantity and intensity in the upcoming decades. In catchments affected by ore mining, flooding leads to the deposition of fine sediments enriched in trace metal(loid)s. Depending on their concentration, trace metal(loid)s can be a health hazard. Therefore, exposure of the local population to flood sediments, either by ingestion (covering direct ingestion and consuming food grown on these sediments) or via inhalation of dried sediments contributing to atmospheric particulate matter, is of concern.

Results The extreme flood of July 2021 deposited large amounts of sediment across the town of Eschweiler (western Germany), with the inundation area exceeding previously mapped extreme flood limits ($HQ_{extreme}$). These sediments are rich in fine material (with the < 63 µm fraction making up 32% to 96%), which either can stick to the skin and be ingested or inhaled. They are moderately to heavily enriched in Zn > Cu > Pb > Cd > Sn compared to local background concentrations. The concentrations of Zn, Pb, Cd, Cu, and As in flood sediments exceed international trigger action values. A simple assessment of inhalation and ingestion by humans reveals that the tolerable daily intake is exceeded for Pb. Despite the enrichment of other trace elements like Zn, Cu, Cd, and Sn, they presumably do not pose a risk to human well-being. However, exposure to high dust concentrations may be a health risk.

Conclusions In conclusion, flood sediments, especially in catchments impacted by mining, may pose a risk to the affected public. Hence, we propose to (I) improve the flood mapping by incorporating potential pollution sources; (II) extend warning messages to incorporate specific guidance; (III) use appropriate clean-up strategies in the aftermath of such flooding events; (IV) provide medical support, and (V) clue the public and medical professionals in on this topic accordingly.

Keywords Flood-related sediment deposition, Contamination, Trace metals, Dust, Public health risk, July 2021 flood

*Correspondence:
Alexandra Weber
alexandra.weber@geo.rwth-aachen.de
Full list of author information is available at the end of the article

Graphical Abstract

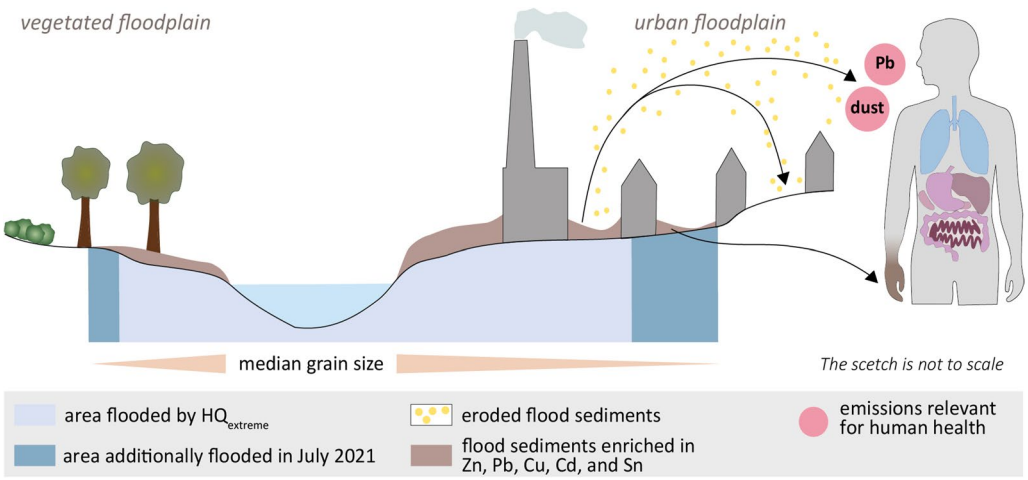

Background

The frequency of extreme flood events is expected to rise due to climate change [1–3]. Among other things, this is worrying because floods are a primary transport mechanism for sediment-related trace metal(loid)s, hereafter referred to as trace metals, from mining and industrial activities [4–7]. Hence, public health risks associated with flooding are also expected to rise [8]. As extreme floods cannot be avoided, the key to adaptation is the implementation of appropriate measures based on a thorough understanding of flood-related processes. Therefore, knowledge of the interaction between flooding and sediment dynamics is of importance to prevent floods from becoming disasters [9].

Flood-related sediment-bound trace metal transport

Pollutant mobility is the net result of mobilizing and stabilizing factors acting on a sediment [10], with floods being a main driver for hydraulic mobilization. Strong currents have especially large entrainment and transport capacities, resulting in large amounts of sediments and debris deposition when flow velocities start to reduce, for example, on floodplains [11]. Flash floods are characterized by high-intensity rainfalls in areas with high topographic gradients, resulting in steep flood waves with only a short warning time. They have a particularly high potential to trigger exceptional geomorphic processes, like bank erosion, slope failure, and surface erosion [12, 13]. This results in intensified sediment transport and, in turn, intense sediment deposition in areas with gentle slopes or floodplain areas with reduced flow velocities. In inhabited areas, flood sediments are deposited outdoors and indoors in flooded buildings [14]. Particularly basements act as sediment traps.

This deposition of flood sediments can be concerning, as they are often enriched in pollutants. The enrichment of trace metals is of particular interest, as they are largely persistent, non-biodegradable, and many are known to accumulate along the food chain [15]. It has been known for decades that such enrichment poses a risk to human health [16], e.g., when flooded areas are used for crop production [17]. Mining-induced contamination with heavy metals is of exceptional longevity, with over 70% of contaminants remaining within the river system for more than 200 years after mine closure [18].

In areas where ore deposits are exploited, the naturally occurring enhanced concentrations of trace metal that possibly can be harmful to human health can be further anthropogenically increased by orders of magnitudes [19]. There is broad evidence of trace metal enrichment in catchments affected by mining activities [4, 6, 18, 20–30]. They originate from primary sources like mine tailings and dumps, which may be eroded due to runoff [6] or the undercutting of former disposal sites in floodplains [4]. Erosion of fluvial sediments deposited during previous flood events along the river on its floodplains or in the riverbed itself is a secondary source of trace metal-enriched sediments [11, 24, 28, 31, 32]. Weathering of contaminant particles like metal sulfides and the consequent leaching of dissolved trace metals may further contribute to dissolved metals [6, 10], which may reprecipitate when conditions change [11, 33].

Trace metals in rivers are transported mainly bound to silt- and clay-sized particles [23, 34, 35]. Therefore, their

fate is closely linked to those of suspended sediments [11, 15, 36]. Generally, mixing with "clean" sediments leads to a dilution of trace metals during high discharges [37–39]. However, extreme flooding may cause erosion in areas usually unaffected by overflow. Additionally, during flash floods, strong runoff is typical [13], which is the major contributor to river sediments [22]. If strongly polluted sediments get eroded, sediment-bound trace metal concentrations in the water may, in fact, increase [24]. The majority of sediment-bound contaminant transport occurs during high-magnitude floods [25]. Because of the dilution effect, trace metal concentrations are generally the highest proximate to their source [40].

Airborne particulate matter and related health risks

As flood waters transport large amounts of fine-grained materials, which are readily erodible and entrained into the atmosphere, regularly flooded areas are typical source regions of atmospheric dust [41]. For the entrainment of any particle, there needs to be an external force transferring kinetic energy to the particle in question. This momentum can be either air movement, another particle's impact, or mechanical force due to human actions (e.g., dirt road vehicles) [42]. The efficiency of particle mobilization depends on many factors, including the moisture content of the sediment, wind speed, particle sizes, and surface roughness [43, 44]. Once in the air, the time a particle can stay in the atmosphere mainly depends on wind speed or atmospheric instability and its size and shape. Particles up to tens of [µm] can potentially remain in the atmosphere for days [45], with PM_{10} (particulate matter < 10 µm) being in long-term suspension virtually independent of friction velocities [46]. In the context of cleaning in the aftermath of flooding, their erosion is not limited to natural aeolian erosion processes. We assume the cleaning and turbulence induced by human activities to play an important role in the health endangerment of local citizens due to dust stress and the chemical inventory of the sediment.

Hurricane Katrina (2005) is a prominent example of a flooding event causing widespread health issues [47, 48]. The flood sediments covering large parts of New Orleans were resuspended by wind and anthropogenic impacts like vehicles, causing an "inhalation hazard" [49]. The resulting particulate matter (PM) proved to induce pulmonary inflammation in mice [50]. The health impacts of the deposited sediments continued for years [50], with an especially high risk for children [49]. The problem was so widespread that names like "Katrina Cough" or "Flood Crud" were established for related respiratory problems in the aftermath of the hurricane [51].

There is broad evidence for the adverse effects of airborne particulate matter on human health [52], with elevated levels of PM resulting in higher cardiopulmonary morbidity and mortality in exposed populations [53, 54]. Many studies documented increased death rates on days with elevated levels of airborne particulate matter [55–58].

The grain size of the inhaled particles influences the pathological effects. Particles > 10 µm are filtered within the nose. If inhaled through the mouth, which is an ineffective filter [59], they are mostly rejected by expectoration [54, 60]. These particles mainly have adverse health effects if they contain toxic substances [43]. Particles < 5 µm penetrate the pulmonary region [61] and can ultimately be deposited in the pulmonary alveoli [57], where they may induce chronic lung diseases. Particles < 2.5 µm ($PM_{2.5}$) are a particular cause for concern for community health [41]. The actual effects depend on the density, shape, surface area, chemical composition, and persistence of the particle, as well as the exposure [43, 62, 63].

Apart from free crystalline SiO_2, which may induce lysosomal damage and trigger the inflammatory cascade leading to subsequent fibrosis (i.e., silicosis) [64, 65], metals seem to play an important role [63, 66–69]. Many trace metals, like Zn, Cu, Pb, Cd, and Ni, are common in PM [45], and fine sediments may act as a sink and, consequently, as a secondary source of these contaminants [70, 71]. Costa and Daniel [72] found that the dose of soluble transition metals determined the acute inflammatory response. However, the mechanisms are still not fully understood. It is shown that metals can have geno- as well as neurotoxic effects [73–75], mediate the production of reactive oxygen species, which induce oxidative stress in cells and tissues [76–78] and cause cell damage [67] and inflammation [66, 79]. These effects are not limited to heavy metals, as it was shown that exposure to aluminum-enriched dust increases the risk of dementia and cardiovascular disease [80]. Additionally, metals have the potential to accumulate in fatty tissues, thus, posing a long-term health risk [62]. Metal exposure mostly encompasses several metals, so their interactions are crucial [81]. They range from joint toxic actions to some metals having a protective function against others. However, these complex interactions are poorly understood so far [69, 82, 83].

Aim of the study and research questions

This study aims to assess the risks posed to the residents of Eschweiler, a town in western Germany severely affected by extreme flooding in July 2021. In the aftermath of this event, clean-up efforts of houses, basements, and streets were conducted with little to no suitable protection equipment. Hence, involved persons were exposed directly to large amounts of flood sediments.

However, the first warnings concerning possibly polluted sediments and dust stress emerged days after the flooding (e.g., [84]), leaving affected people uninformed for days.

To evaluate the risk posed by the fine sediments to the residents and first responders, detailed insight into the deposition of sediments and their properties, including a possible enrichment of risk elements and their possible toxic effects, is necessary. Therefore, we conducted numerical modeling of the flood-related sediment transport within the densely populated city of Eschweiler and combined the results with geochemical and grain size data on samples of the flood sediments. Anthropogenically induced enrichment of trace metals is identified by comparison with background concentrations. Furthermore, a simple estimation of the daily intake of sediments allows for determining trace metals posing a risk to human health.

Methods

The July 2021 flood event

Unprecedented rainfall between July 14th, and July 15th, 2021, led to a flooding crisis in the German and Belgian Eifel region. The largest part of the Eifel-Ardennes received approximately twice the amount of their monthly precipitation within only 2 days, resulting in major flooding of all rivers draining the low mountain range [85]. Maxima of rainfall were >150 mm within 24 h [86], with many stations recording their all-time maximum precipitation [87]. The amount of precipitation exceeded an event with a return period of 500 years [88].

The Eifel-Ardennes are part of the variscan Rhenish Massif, consisting of plateaus with steeply incised fluvial valleys. On top of the bedrock, which in the Eifel region is made up mainly of intensely consolidated sedimentary rocks, there is a layer of unconsolidated periglacial material that builds the parent material for soil development, mainly forming cambisols [89]. They commonly have a high skeletal content, which lowers their water storage capacities [90]. The persistent rain quickly saturated the soils, which were already strongly waterlogged due to previous rainfall [86]. Saturation conditions of the sediments are a crucial driver for flash flood generation [91].

The combination of intense rainfalls, topography, and saturated soils led to a flooding crisis [90], affecting large areas of western Germany, Belgium, Luxemburg, France, and the Netherlands. In Germany, more than 180 people died, and financial losses added up to approximately 33 billion Euros [92]. The destruction of infrastructure and houses was severe [93] and persisted in part up until one and a half years later. Due to the extremely high water levels, the floodplains were affected even in areas that were assumed to be safe [93], and the deposition of flood sediments was widespread.

While research [88, 94–96] and reports [97] focus on the shocking amounts of debris transported by the rivers, ultimately exacerbating the event by clogging bridges that failed later on, little attention has been paid to the fine fraction of the flood sediments. However, as the transport capacity for fine materials is particularly high, they are spread over larger areas. As a result, even the outer parts of the flooded areas, which are not affected by debris, were covered by a thin, continuous layer of fine sediments.

Study area

The town of Eschweiler, located at the Inde River, a main tributary of the Rur, was also severely affected by the flood. In the city center, critical infrastructure was disturbed: the hospital's basement was flooded, leading to the evacuation of 300 patients, the collapse of the power supply, and the destruction of the building technology [98].

The source region of the 54-km-long Inde river is in Belgium on the northern slope of the High Fens. The catchment area of the Inde River covers 344 km^2. Its course is dominated by the geologic underground, which consists dominantly of high-angle dipping Devonian and Carboniferous sedimentary rocks. Near the city of Eschweiler, it crosses the border from the low mountain ranges of the Eifel to the lowlands of the Lower Rhine Embayment (see Fig. 1). In the further course, the underground is dominated by quaternary sediments like gravel, sand, and loess [99, 100]. Responding to several flood events, the Inde was canalized in the town center of Eschweiler in the 1970s as a flood protection measure [101]. The gradient was set at 1.2–1.8‰ with the help of bed slides, and a double-trapezoidal profile was chosen for a design water discharge of 150 m^3/s.

Eschweiler is located along the part of the Inde River, which exhibits the highest trace metal concentrations in sediments [102]. The underlying strata of the Devonian and Carboniferous are famously known for their intense metallization. zinc, iron, and lead mining date back to Roman times but had their height during late industrialization. Legacies of these mining activities resulted in fluvial sediments being severely enriched in trace metals like Ni, Cu, Zn, As, Cd, Sn, and Pb [103]. Additionally, the waters of the Inde in Eschweiler and the immediately upstream located city of Stolberg have been documented to be enriched in Tl, Zn, As, Co, Cu, V, and Cd [104]. Mining of local hard coal deposits in the area of Eschweiler is another source of trace metals. As a result, Eschweiler was dominated by heavy industries, some of which are still operating [103].

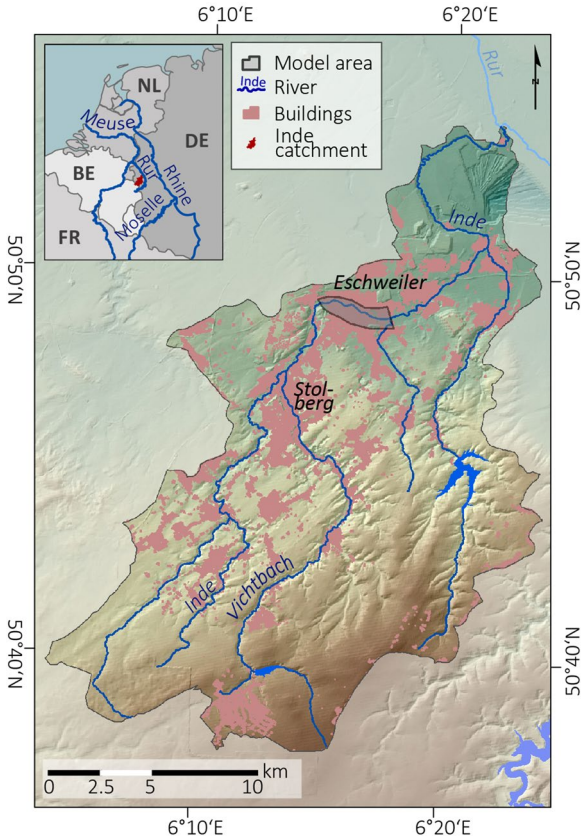

Fig. 1 Overview of the Inde catchment. The grey area in the main map indicates the area of the Delft 3D-Model. All flood sediment samples are taken in the city of Eschweiler. Samples for background assessment were collected along the uppermost reaches of the Inde river. FR: France; BE: Belgium; NL: The Netherlands; DE: Germany

Sampling

Flood sediment sampling was conducted on several days from July 18th to August 4th, 2021. Suitable sampling locations where fine sediments might have accumulated were identified based on the official flood risk maps. Based on visual differentiation, only uncovered, apparently freshly deposited sediments were sampled to ensure they were, in fact, deposited by the flooding. The samples were stored in plastic Whirl-Paks® or glass containers and refrigerated until further analytic work. Of the overall sampling set (150 samples), 12 samples were taken in the city of Eschweiler and selected for analysis in this study (see Fig. 2).

Additionally, to assess the enrichment of trace metals in the flood sediments with respect to the geogenic background, topsoil samples from the floodplains of the uppermost reaches of the Inde river were collected. In this reach, anthropogenic impact on the Inde river is minimal. In Belgium, the area is mainly used for forestry, and in Germany, the Inde flows through an inhabited protected landscape. To further minimize the anthropogenic impact on the geochemistry of the floodplains, sample collection was limited to the reaches upstream of the uppermost mill at the Inde River, from where the human impact on the river gradually increases. This second sampling set contains 18 samples collected by extracting cubes with an edge length of 20 cm using a spate. These cubes were sampled evenly along the 20 cm depth.

Laboratory analysis

Grain size composition was obtained by laser diffraction measurement following the routine described in detail by Schulte et al. [105]. Samples were dried at 35 °C before gently ground in an apatite mortar and sieved to < 2 mm. To remove organic matter, the sediment was repeatedly treated with 0.70 mL 30% H_2O_2 at 70 °C for several hours until the material showed bleaching. Samples were additionally treated with 1.25 mL $Na_4P_2O_7$ (0.1 mol/L) overnight using an overhead shaker to ensure the dispersion of particles [106, 107]. Laser diffraction measurement was conducted using a Beckman Coulter LS 13,320. The resulting 116 grain size classes giving the percentage size frequency of particles from 0.04–2000 µm with an error of 2% were used to calculate concentrations of health-relevant classes like $PM_{2.5}$ and PM_{10}. Calculation of grain size distribution followed Mie theory (Fluid RI: 1.33; Sample RI: 1.55; Imaginary RI: 0.1) [105, 108, 109].

Following the suggestions by Babek et al. [110], elemental concentrations were determined using the complete sample material with particle sizes < 2 mm, relinquishing the common sieving to < 63 µm for trace metal analysis. Samples were dried at 105 °C in a drying cabinet and afterward sheared for 2 min in a planetary mill. Next, 8 g of the so-obtained material were mixed with 2 g Fluxana Cereox binder, homogenized by shaking, and pressed to a pellet by applying a pressure of 19.2 MPa for 120 s. Elemental composition was measured by energy-dispersive polarized X-ray fluorescence (XRF) (Spectro Xepos) in duplicate, and their arithmetic means were used for further analysis [111].

Statistical analysis of trace metals

Besides anthropogenic enrichment, trace metal concentration in sediments depends on various factors, mainly grain size distribution, source-rock composition, and the degree of soil weathering [112]. Therefore, it is necessary to gain an understanding of these naturally occurring variabilities in trace metal concentrations to distinguish them from anthropogenic influences [35].

Floodplain samples from the upper Inde catchment were used to assess the local background concentrations to gain insight into the anthropogenic enrichment

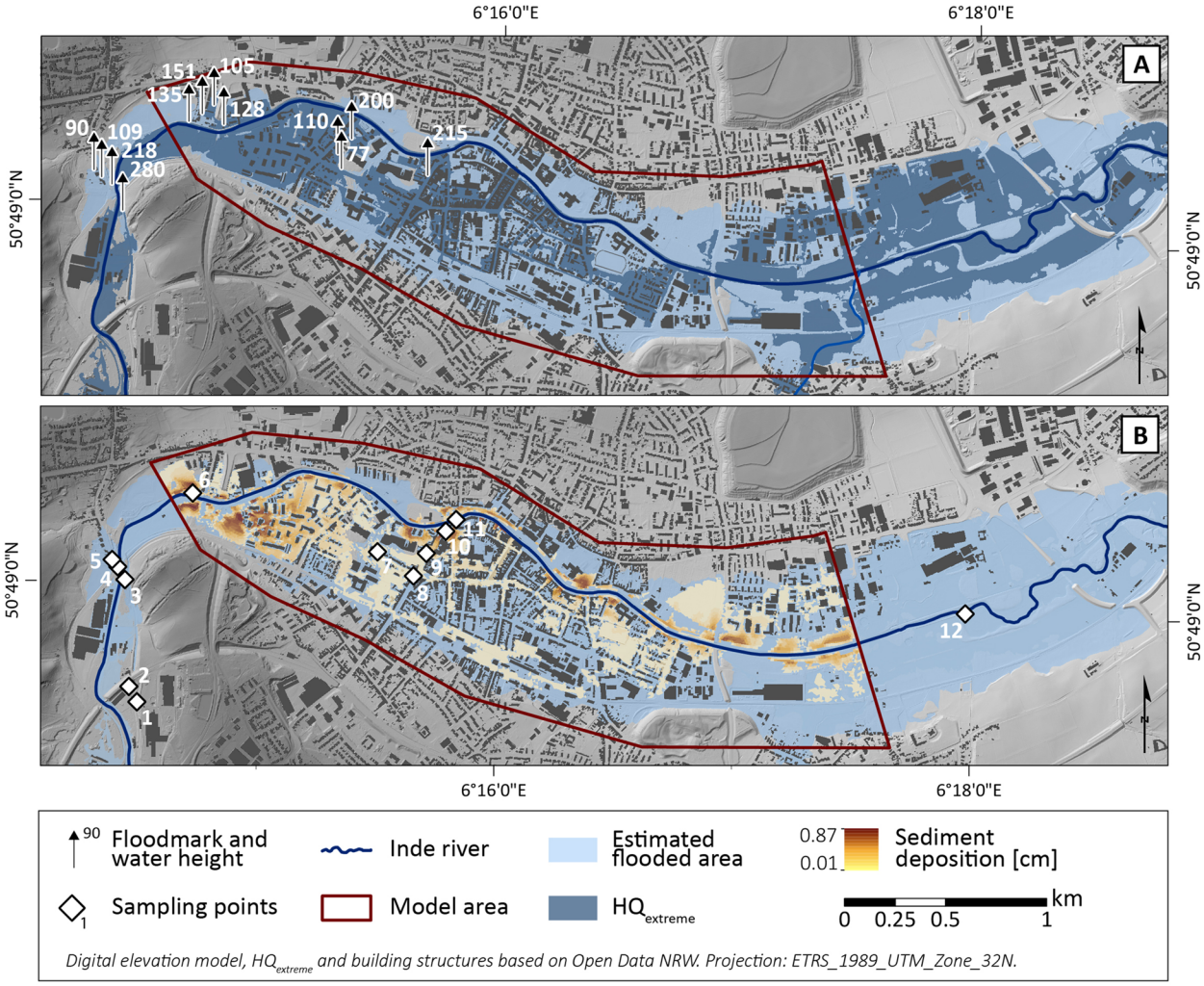

Fig. 2 Sediment accumulation and flooding within the focus area. Map **A** provides the inundation area (light blue), which exceeds the previously mapped extreme flood limits (darker blue). Additionally, all floodmarks are given. Map **B** provides the modeled sediment accumulation in the same area. The yellow-brownish colors indicate sediment deposition, with darker shades implying more intense sediment deposition. The red line gives the limits of the area included in the sediment deposition model. The blue color indicates a reconstruction of the areas flooded in July 2021. Additionally, all sampling points are given. Only the 6 sediment samples collected within the model area, as indicated by the red line, were used for the model

of trace metals [113, 114]. This sampling setup aims at identifying a baseline or "usual background value", which, in addition to the geogenic background, also implies diffuse anthropogenic inputs like atmospheric deposition. It, therefore, differs from a pure "natural background value" [112]. Usually, methods based on robust regressions are best suited to account for background concentrations of trace metals [114, 115]. However, no satisfactory regressions were found between the trace metals of interest and the typical lithogenic elements usually used for normalization, e.g., Zr, Al, Ti, and Rb [110, 115]. Therefore, a univariate approach had to be implemented. The iterative 2σ-approach following Mattschullat et al. [116] was applied to estimate the background concentrations of all elements measured using XRF. An iterative approach is beneficial because the regular 2σ-approach assumes normally distributed concentration values, which is usually not the case in a geochemical context. Instead, log-distributions are more common for trace metal concentrations in floodplain sediments. By switching to an iterative approach, this issue is addressed by a step-by-step generation of a normal distribution. The $\overline{x}+2\sigma$ ($\overline{x}$ indicating the arithmetic mean) is calculated using the whole sample set (including all possible outliers). All concentrations

exceeding this value will be excluded from the next calculation. This procedure gets repeated until all concentration values lie within the $+2\sigma$-range. The $\bar{x}+2\sigma$ based on this population is used as natural background concentration. This approach is suitable for analyzing typical heavy metal(loid)s [116].

These background concentrations build the basis to assess the enrichment of trace metals in the flood sediments. A classic enrichment factor (EF) with aluminum as a reference element was calculated to identify elements with a concentration higher than expected based on their background concentrations:

$$\mathrm{EF} = \frac{\mathrm{TM}_{\mathrm{sample}}/\mathrm{Al}_{\mathrm{sample}}}{\mathrm{TM}_{\mathrm{ref}}/\mathrm{Al}_{\mathrm{ref}}} \quad (1)$$

with $\mathrm{TM}_{\mathrm{sample}}$ and $\mathrm{Al}_{\mathrm{sample}}$ being the concentration of any trace metal and aluminum in the sample, respectively, and $\mathrm{TM}_{\mathrm{ref}}$ and $\mathrm{Al}_{\mathrm{ref}}$ indicating their concentrations in the chosen background [117]. An EF > 1 indicates enrichment of the analyzed elements compared to their background. However, this evaluation strongly depends on the chosen baseline, and values close to unity might derive from naturally occurring fluctuations but still be considered enriched [117].

Additionally, to compensate for the mentioned limitations of the EF and to evaluate the intensity of contamination in an intelligible way, we calculated the commonly applied geoaccumulation index I_{geo} introduced by Müller [118] using the following formula:

$$I_{\mathrm{geo}} = \log_2\left(\frac{C_n}{1.5B_n}\right), \quad (2)$$

where C_n is the measured concentration of a trace metal within a sample and B_n is the background concentration of this specific element.

The underlying local background is based on samples from an area not underlain by mineralized limestones. Therefore, the enrichment factors calculated in this study reflect not only anthropogenic activities, but also enrichment due to naturally occurring ores. However, due to the catchment being densely populated, the areas underlain by metal-enriched limestones did not remain in a natural state, and hence, they are not suited for evaluating the geogenic background. Therefore, the upper Inde still seems to offer the most appropriate option.

Trace metal exposure

A rough estimation of daily exposure was conducted, assuming a daily intake of 90 mg of soil and 100 mg of dust for an adult, as suggested by US EPA [119], resulting in a total daily intake via inhalation and ingestion of 190 mg of sediment. This estimation is the upper percentile rate to account for the extensive exposure to sediment in the aftermath of the flooding event. We only know concentration values for bulk samples, so we assumed constant concentrations for all grain sizes, resulting in a lower-end estimation, as many studies report higher concentrations of trace metals in the fine fraction [59, 120–122]. This conservatively estimated uptake was compared to the probable tolerable daily intake (PTDI) levels by the Joint FAO/WHO Expert Committee on Food Additives (JECFA).

Delft 3D FM model

The program Delft3D FM was used to model sediment transport during the July 2021 flood event in Eschweiler. The 2D-model incorporates depth-averaged velocities, at which the river is modeled with rectangular grid cells, and the floodplains are mapped with triangular cells. In total, the grid covers an area of 3.62 km^2 and consists of a total of 44,468 cells and 24,007 nodes. The average size of the cells is 72.24 m^2, with the smallest cell covering an area of 9.86 m^2 and the largest an area of 312.63 m^2. The grid has a grid width of 3.25 m to 28.2 m with a maximum orthogonality of 0.382 and an aspect ratio ranging from 1 to occasionally 4.19.

The bathymetry is based on a DEM 1, and the river tube was deepened by 1.3 m. This value was obtained by looking at the cross-sections of the Inde in the study area. Additionally, buildings were added to the DEM. An inflow hydrograph, the inflow over time, serves as the inlet boundary condition, and the water level as a function of the flow serves as the output boundary condition.

For the value of the Chézy friction coefficient, 31 $m^{1/2}/s$ was set when calibrating the model based on the flood risk maps [123–125] with a reference discharge of 185.3 m^3/s at a water level of 3.4 m. The water levels on the floodplains varied by less than 0.1 m on average.

During the flood incident in mid-July 2021, a maximum water depth of 3.7 m was measured at the gauging station Eschweiler, but the corresponding discharge is unknown. Thus, an equivalent maximum flood wave discharge of 270 m^3/s was estimated and applied over 6 h, representing the peak of the flood wave from July 15th 2021, at 03:30 am to 09:30 am. Peak water depths in the model matched flood mark heights with a mean accuracy of 17 cm.

The sediment transported in the model consists of 6 fractions. These fractions each reflect the mean value of the grain sizes of the six sediment samples collected within the area defined for the numerical model;

samples 6 to 11 (see Table 1). Their sinking velocity was calculated after Cheng [126]. An initial thickness of the sediment layer of 2 cm was assumed because the study area is mostly asphalted. The critical bed shear stress for sedimentation on the foreshore was set at 1000 N/m^2 and in the river channel at 1 N/m^2. The critical bed shear stress for erosion in the river tube was assumed to be 45 N/m^2 after Maaß and Schüttrumpf [127], who determined the bed shear stress for erosion in the river bed of the Wurm River for long-term modeling. The value from the Wurm River, a tributary to the Rur River following downstream of the Inde River which holds the same river typology as the Inde River, was applied, since the Inde River is not wadable in the section of our study area and therefore, bed samples cannot be collected with reasonable effort.

Table 1 Sediment characteristics for the numerical model

Sample	Mean diameter (µm)	Corresponding settling velocity (cm/s)
6	94.78	0.593
7	104.57	0.713
8	69.73	0.341
9	31.74	0.079
10	90.98	0.553
11	91.25	0.556

Mean sediment diameters of samples incorporated into the numerical modeling and their corresponding settling velocity after Cheng [126]. Only the sediment samples taken from the defined model area were incorporated into the model, i.e., samples 6 to 11

Results

Flooded area and sediment deposition

The reconstructed inundation area, as derived from the flood marks and the DEM 1, significantly exceeded the previously mapped area for a rare flooding event (see Fig. 2). Flood control design dimensions are clearly exceeded resulting in the flooding of large parts of the floodplain, much of which is occupied by built-up areas belonging to the city of Eschweiler.

The numerical model provided the probable thickness of the accumulated sediment layer deposited by the July 2021 flood (see Fig. 2). Almost the entire inundation area was covered by a thin sediment layer of less than 10 cm.

Areas with large sediment accumulations (>40 cm) were banks on impact slopes, areas next to bridges, low-lying areas such as fields, car parks or field paths, a ditch running parallel to the Inde river, and where the water current encounters barriers like buildings. In these areas, the model output predicted sediment thicknesses of 40 to 60 cm and, occasionally, up to 87 cm.

Erodible flood sediments

The readily erodible silt- and clay-sized fraction (i.e., particles < 63 µm) made up 32% to 96% of the sediment

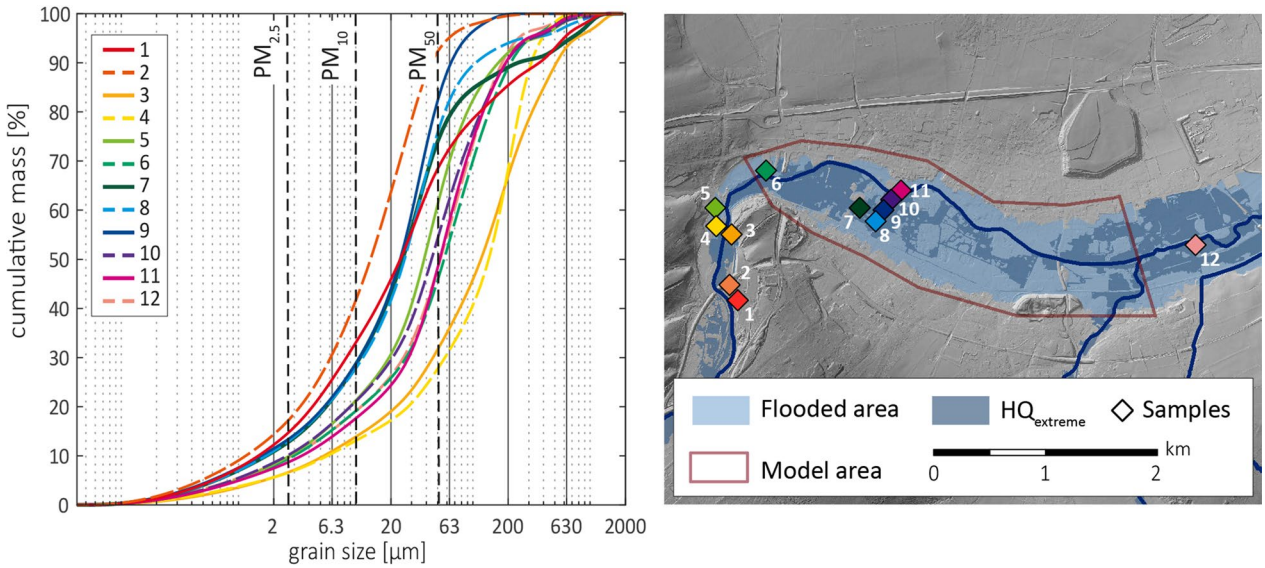

Fig. 3 Sum curves of grain size for all flood samples. The dashed black lines give the limits of $PM_{2.5}$ and PM_{10}, respectively. All sampling points are depicted in the map on the right. The dark blue area in the map indicates the inundated area in case of an extreme event (return period of significantly more than 100 years). The light blue colored area indicates the modeled inundation area for July 2021, which exceeds the designated inundation area of an extreme event

samples (Fig. 3). PM_{10} and $PM_{2.5}$ accounted for 13% to 42% and 6% to 17%, respectively. Even though PM_{10} is the standard for assessing inhalation exposure, Goix et al. [120] recommend considering all particles < 50 µm for the evaluation of exposure to prevent underestimating the exposure of children, mainly because children display intense hand-to-mouth activities, which is a crucial exposure route in terms on ingestion of sediment. In our study, PM_{50} varied between 28 and 92% (see Table 2). All samples showed a distinct maximum of their grain size distribution for silt-sized particles. However, samples 3 and 4 contained significant amounts of sand (63% and 68%, respectively), whereas sample 2 generally had the highest amount of fine material. All these samples were taken upstream from the city center. Samples collected within the city center of Eschweiler (samples 6–11) were in between these extremes.

Especially for medium to coarse silt, there seemed to be a trend for the samples to be less enriched in finer material if collected in the vicinity of the river channel. This coarsening is related to higher flow velocities close to the channel resulting in higher transport capacity for finer materials. Contrary, distant from the channel, also the finest materials are deposited. This effect was evident for the finer samples 7, 8, and 9 versus samples 10 and 11, collected nearby but much closer to the channel. However, the very local morphology of the sampling spot played an important role. This effect was apparent for samples 1 and 2. The much finer sample 2 was taken from a small depression, whereas sample 1 was collected next to a minor road, which enabled higher flow velocities.

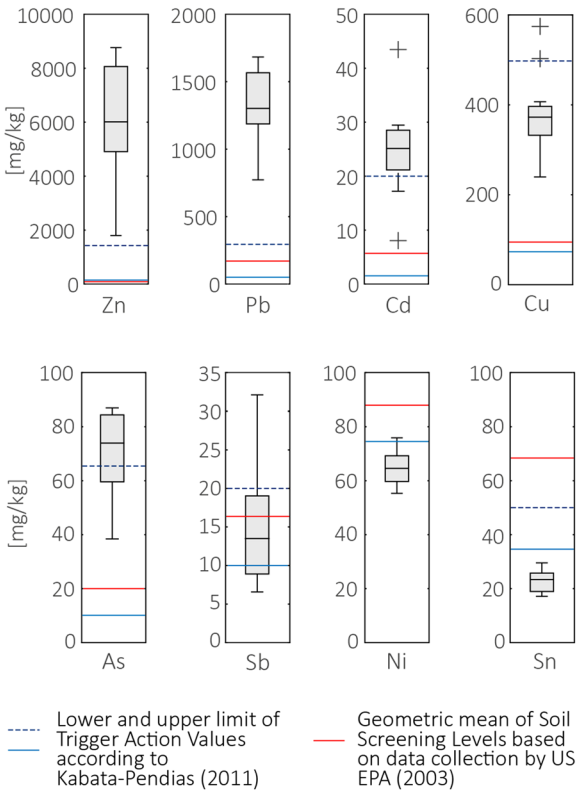

Fig. 4 Boxplots of the absolute concentrations of trace metals, which showed enrichment over their background concentrations. All concentrations are given in mg/kg. Blue lines indicate the upper and the lower limit of the trigger action values as collected by Kabata-Penidas [128] from several European legislative documents. The upper limit for Ni exceeds the range of the plot. The red line indicates the geometric mean of screening levels compiled by the US EPA [129] from legislative documents with a focus on North America

Trace metal enrichment in flood sediments

We focussed on health-relevant trace metals exhibiting an enrichment over their background concentrations, i.e., EF > 1 for all samples. This statement was true for eight metal(loids), which were enriched in the following order Zn > Cu > Pb > Cd > Sn > As > Sb > Ni (see Table 2). For absolute mean concentrations, the order was Zn > Pb > Cu > As > Ni > Cd > Sn > Sb (see Fig. 4). This highlights the relevance of Zn, Pb, and Cu in the Inde catchment. Zn and Pb were mined for centuries and built the basis for intense industrial development. Even though Cu was imported in large parts, it was an essential raw material for the brass industry in Stolberg, upstream from Eschweiler [102].

A somewhat simple and easy-to-implement assessment of the trace metal-related risk is the comparison of metal concentrations with threshold concentrations. Here, the trigger action values as collected by Kabata-Penidas [128] from several European legislative documents as well as Screening Levels compiled by the US EPA [129] from North American legislative documents were consulted. Figure 4 shows boxplots of the concentrations of the relevant trace metals together with critical values for their concentration. For Zn and Pb, all samples exceeded the upper boundary of limits severely. Depending on the applied limit, Cd, Cu, and As also exceeded the threshold concentrations for most or all samples. The concentrations of Sb were in the range of the limits. Ni and Sn mostly did not exceed the concentration limits, even though they were enriched compared to the background.

The I_{geo}, which is based on enrichment over background concentrations, addresses the question of pollution independent of ecologically defined threshold levels. For its interpretation, it is important to keep in mind its logarithmic character, resulting in each class implying a doubling of enrichment over background concentrations. The resulting seven classes rank trace metal concentrations from practically uncontaminated to extremely contaminated.

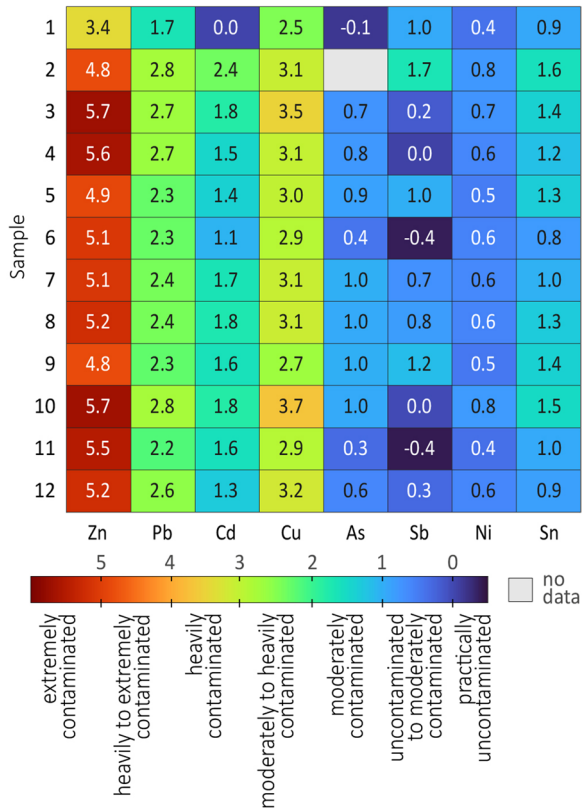

Fig. 5 Heatmap of the I_{geo} for the enriched trace metals in samples 1 to 12. Note the logarithmic character of the I_{geo}. Contamination is evident for Sn, Cd, Pb, Cu, and Zn. For Ni, Sb, and As, enrichment over the background concentration is insignificant, resulting in an I_{geo} below 1

The samples were heavily to extremely contaminated with Zn, with most of the samples being heavily contaminated ($I_{geo} > 5$) (see Fig. 5). Samples 3 and 10 reached a maximum of $I_{geo} = 5.7$. Müller [118], when introducing the I_{geo}, stated that, even though the uppermost class has no upper limit, the I_{geo} will exceed a value of 6 in riverine sediments only on rare occasions. This highlights the intensity of the Zn contamination. The I_{geo} for Cu ranged between 2.5 and 3.7, indicating mostly heavy contamination. Pb showed moderate to heavy contamination, having an I_{geo} between 1.7 and 2.8. Even though Cd exceeded the trigger action levels (Fig. 4), it resulted only in moderate contamination (Fig. 5). Sn showed moderate contamination, presumably linked to the float glass production using tin baths, which is common in Stolberg's glass industry [130]. For As, Sb, and Ni, the I_{geo} was mainly < 1, indicating no contamination with these trace metals. Even though they were enriched compared to the background, as indicated by the enrichment factor > 1, the I_{geo} suggested no contamination due to multiplying the background concentration by a factor of 1.5 (see formula 1). There were no clear trends apparent when comparing the samples to each other. Noteworthy, the relatively coarse samples 3 and 10 seemed to contain the highest level of contamination.

Trace metal exposure

Daily intake of the analyzed trace metal based on estimated daily ingestion of 190 mg of soil and dust, along with their PTDI, is listed in Table 3. For most elements, the modeled daily intake was within limits defined by the WHO. Some trace metals and their compounds are essential for the life of plants, animals, and humans, resulting in high tolerable daily doses for some compounds [128]. Only the modeled intake of Pb exceeded the PTDI for those samples with high Pb concentrations. This applies to samples 2, 3, 4, 10, and 12. Though, following the most recent WHO updates, no safe level of exposure could be identified for Pb and As. Therefore, exposure to these elements is of concern as a matter of principle. However, as the intake of As was below the outdated threshold level, we assume that only Pb was of major concern (Table 3).

Discussion

Risk assessment

The I_{geo} indicates contamination of the flood sediments by Zn, Cu, Pb, Cd, and Sn. This enrichment in several trace metals is not unexpected, as the simultaneous enrichment of Pb, Cd, and Zn is common for zinc smelting areas [71] like the Inde catchment. The resulting industrial development leads to multi-element contaminations typical for regions with long industrial history [121]. Other relevant industries besides the coal and steel industry, some of which are still located in Eschweiler and Stolberg today, were glass production, the pharmaceutical industry, the chemical industry such as detergent production, and the textile industry [138]. These industries settled preferably to use the water on the Inde and Vicht rivers [103]. Sewage treatment plants, another typical source of trace metals, mainly emit Hg, Cu, Cd, Zn, Pb, Cr, and Ni [139]. The Stolberg-Steinfuhrt wastewater treatment plant is located immediately upstream of Eschweiler in Stolberg and discharges treated wastewater into the Inde river. In the Inde catchment, the average amount of zinc in stormwater collected for treatment is 0.62–2.38 t/a and of copper 0.09–0.36 t/a [140].

However, the absolute concentrations of trace metals found in the flood sediments in Eschweiler exceed the values reported by Esser et al. [102], who investigated channel sediments from the Inde River. This implies additional pollution sources that are usually not part of the fluvial sediment system. Undercutting and subsequent

Table 2 Results of XRF-measurement, EF calculation, and grain size analysis for all flood samples

Sample *N°*	1	2	3	4	5	6	7	8	9	10	11	12	$\bar{x}+2\sigma$-background
Absolute concentrations (mg/kg)													
c(Al)	48,645	64,900	50,310	55,550	52,145	53,825	58,410	56,045	54,280	55,675	47,450	56,835	82,564.0
c(Ni)	56.1	73.1	70.9	64.9	60.4	63.1	66.7	63.8	58.6	75.3	55.2	64.8	28.5
c(Cu)	241.1	375.2	498.1	366.9	358.0	331.5	374.8	384.1	284.6	568.2	331.5	404.7	29.0
c(Zn)	1797.0	4844.5	8760.0	8420.5	4971.5	5635.0	5772.5	6246.5	4812.0	8586.5	7704.0	6294.0	112.3
c(As)	38.7		71.8	73.4	79.6	57.6	85.9	83.7	86.1	83.4	54.0	64.8	28.6
c(Cd)	8.1	43.5	29.5	22.8	21.7	17.2	26.3	28.0	25.3	29.1	25.0	20.7	5.5
c(Sn)	18.5	29.0	25.2	21.9	24.6	16.9	19.8	24.0	25.4	27.9	18.9	17.7	6.4
c(Sb)	19.2	32.2	11.1	9.5	19.9	7.6	16.3	17.7	22.3	10.0	7.5	12.2	6.6
c(Pb)	772.4	1633.0	1583.5	1548.0	1204.5	1228.5	1298.0	1306.0	1169.0	1683.0	1100.5	1467.5	161.6
Enrichment factor with Al as reference element													
EF(Ni)	3.3	3.3	4.1	3.4	3.3	3.4	3.3	3.3	3.1	3.9	3.4	3.3	
EF(Cu)	14.1	16.5	28.2	18.8	19.6	17.5	18.3	19.5	14.9	29.1	19.9	20.3	
EF(Zn)	27.2	54.9	128.0	111.5	70.1	77.0	72.7	82.0	65.2	113.4	119.4	81.4	
EF(As)	2.3		4.1	3.8	4.4	3.1	4.2	4.3	4.6	4.3	3.3	3.3	
EF(Cd)	2.5	10.0	8.8	6.1	6.2	4.8	6.7	7.5	7.0	7.8	7.9	5.4	
EF(Sn)	4.9	5.7	6.4	5.0	6.0	4.0	4.3	5.5	6.0	6.4	5.1	4.0	
EF(Sb)	4.9	6.2	2.8	2.1	4.8	1.8	3.5	3.9	5.1	2.2	2.0	2.7	
EF(Pb)	8.1	12.9	16.1	14.2	11.8	11.7	11.4	11.9	11.0	15.4	11.8	13.2	
Grain size distribution													
Mean (µm)	111.7	21.9	217.6	158.4	81.4	94.8	104.6	69.7	31.7	91.0	91.2	86.6	
Mode (µm)	34.6	28.7	185.4	223.4	45.8	72.9	34.6	38.0	38.0	50.2	60.5	72.9	
Median (µm)	25.1	14.0	122.6	142.6	40.2	59.4	26.3	27.4	25.1	46.5	54.7	55.2	
$PM_{0.1}$ (%)	0.4	0.5	0.2	0.2	0.3	0.3	0.4	0.4	0.4	0.3	0.3	0.3	
$PM_{2.5}$ (%)	14.3	16.7	6.5	6.4	9.6	9.2	12.5	12.6	13.0	9.9	8.5	9.4	
PM_{10} (%)	33.5	42.3	14.0	13.2	21.5	19.3	29.0	28.2	29.2	21.3	17.8	19.3	
PM_{50} (%)	68.5	92.4	31.7	27.8	61.3	45.9	74.1	75.9	82.4	54.4	48.4	48.3	

Concentrations of all trace metals analyzed in further detail along with concentrations of Al are given for all samples and the calculated background baseline. The selection of the tace metals is based on their EF being > 1 for all samples. Additionally, the grain size statistics are given, including the percentage of health-relevant size classes

failure of river banks was a commonly observed result of the flood [88]. Due to the many legacies in the floodplains of the region, this is expected to lead to an intense input of trace metals into the system [4]. Regular flooding washes off unconsolidated sediments which are prone to erosion due to missing vegetation or weathering. Once this sediment is flushed away, no readily available sediment is left, and the discharge might increase further, but the sediment load declines [38]. Extreme flood events cross certain thresholds, which enable the erosion of far larger amounts of sediments, e.g., by lateral erosion of the river bank [141]. As soon as this process starts, large amounts of erodible sediments are exposed to strong currents. In case also coarser grain sizes, such as gravel or boulder get eroded, this might further accelerate erosion.

The flood sediments deposited in Eschweiler are severely enriched in Pb, and concentrations were many times higher than the upper limits of trigger action values. This result is of special concern as no level of Pb exposure is assumed to be safe [131, 142]. A large part of the exposure of the public to Pb results from the resuspension of contaminated soils [70]. This finding is supported by the fact that blood Pb levels in children correlate with weather conditions, e.g., warm and dry weather aggravates soil resuspension [70]. For several American cities, the resuspension of fine materials was found to be the main source of atmospheric Pb [143]. While the acute toxicity of Pb was low, the long-term effects are of worrying relevance [131]. Therefore, the general enrichment of Pb in surface sediments within the Inde catchment is of even more concern than the exposure to the moderately to heavily contaminated flood sediments (I_{geo} ranges between 1.7 and 2.8). However, floods play a major role in exposure because they induce erosion, redistribution, and the deposition of fine materials in inhabited areas.

Even though absolute concentrations were low, the enrichment of As in flood sediments is of concern for

Table 3 Daily intake of trace metals along with their PTDI levels

Trace element	Daily dose of ingested trace elements (mg/day)		Probable tolerable daily intake (mg/day)[b]
	Min[a]	Max[a]	
Pb	0.147	0.320	*0.268*[c] [131]
As	0.007	0.016	*0.161*[c] [132]
Cd	0.002	0.008	0.075 [133]
Sb	0.005	0.320	0.450 [134]
Ni	0.010	0.014	0.975 [135]
Zn	0.341	1.664	75 [136]
Cu	0.046	0.108	37.5 [136]
Sn	0.003	0.006	150 [137]

The intake levels are based on recommendations by the JECFA, except for the nickel PTDI, which is suggested by the European Food Safety Authority's Panel on Contaminants in the Food Chain. The listed PTDI levels for Pb and As are old levels withdrawn by now, as no safe level of exposure can be identified

[a] Minimum and maximum dosage are derived from the minimum and maximum concentration of each trace metal over all samples, respectively

[b] Assuming an average body weight of 75 kg

[c] Italic writing indicates withdrawn intake levels, no health-protective value can be established

human health. Uptake of As from soil and dust is a well-known phenomenon linked to shortness of breath, cough, and chest pain [19], with long-term exposure being carcinogenic [132]. Similar to Pb, no safe level of As exposure can be specified [132]. However, the I_{geo} indicates no anthropogenic enrichment for As. Therefore, exposure to As is only due to high background concentrations that already exceed trigger action values (see Fig. 4). Again, flooding is relevant because it enhances public exposure to dust.

The numerical model indicates sediment deposition for large parts of the flooded area, even at the margin of the flooding. Sediment deposition strongly depends on the distance to the channel and objects hindering water flow [26]. Additionally, samples distant from the river channel showed higher amounts of the finest particles. Floods act as mobilization and sorting agents, thereby depositing the finest particles in the outer area of the flooding [26]. Therefore, we assume dust generation to be possibly intense over the whole inundation area, even in areas where only little total sediment was deposited. This is even more true for large areas with sealed surfaces, which are susceptible to erosion due to their smooth surface structure and missing vegetation [46]. Moreover, even areas where coarser sediments were deposited, like, e.g., sandbars, act as source areas for dust [144]. The amount of deposited sediment in the flooding corridor was extreme [96], concordant with our model. In Eschweiler, the uppermost part of the city along the river was especially affected by intense sedimentation. This is because the river valley widens from where the Inde enters the city center of Eschweiler, resulting in reduced flow velocities [26] and because the floodplains are densely populated from here on.

There are generally two paths to consider when looking at exposure to sediments enriched in trace metals. The first one is the inadvertent ingestion of fine particles, which stick to the skin [122]. This is especially problematic for children, who exhibit intense hand-to-mouth activities and have lower tolerances for most trace metals. The second path is the inhalation of fine particles [122], which were resuspended into the atmosphere due to either wind or anthropogenic impact.

Particle size plays a vital role in the exact uptake within the human body because it determines the particle's surface area, which comes in contact with tissues, its ability to stick to the human skin, limits how deep a particle can enter the lungs, and governs the body's capabilities of ejecting the particle [54, 120]. Additionally, larger surface areas lead to higher binding capacities for trace metals and hence higher concentrations within the sediment [114]. As we only did bulk sample analyses, we cannot make any statement on trace metal concentrations within specific size groups. However, several studies found enriched trace metal concentrations in the finest fractions [27, 59, 120–122] or the $PM_{2.5–10}$ fraction [145, 146], raising concerns about elevated concentrations in the respirable particles. Moreover, finer particles tend to have higher toxic potential because, for finer particles, their chemical composition becomes more and more relevant [147]. However, this trend is not unambiguous, as some studies found higher trace metal concentrations in $PM_{2.5–10}$ compared to finer particles [81].

Additionally to the flood sediments outdoors, there also needs to be a focus on sediments deposited indoors, where contact with the sediments and their possibly toxic inventory is especially likely. Large amounts of sediment were deposited in the numerous buildings affected by the flooding, especially in the basements. However, the exposure also extends to non-flooded buildings, as transporting exterior sediments into homes, e.g., due to attachment to shoes and clothing [70], is an important pathway for exposure [148]. In addition, sediments attached to people's skin may be a crucial transport vector from outdoors to indoors. Particles < 63 µm with the potential to adhere to the human skin [149, 150] comprise up to 96% of the material in the flood sediment samples collected in Eschweiler. Subsequently, this sediment may get ingested inadvertently. Particles < 2 µm, which account for 6% up to 15% of the flood sediment samples, can even get incorporated into the skin's surface [122]. Therefore, indoor exposure to flood sediment may

persist even after buildings have been cleaned of sediment in the first place.

The concentration of airborne PM indoors is higher than outdoors in the aftermath of flooding events [151]. Moreover, indoor dust tends to accumulate trace metals from outdoor and indoor sources [146]. Additionally, resuspended PM_{10} is proven to be enriched in trace metals compared to settled dust indoors, and resuspension of dust plays a key role in PM levels indoors [146]. Indoor air quality has been shown to be severely deteriorated even months after flooding events and even after full-scale remediation efforts. However, biological particles like mold and fungi have a large share in this [151].

Durational effects are important, as mortality increases for each day with elevated PM_{10} concentrations [56]. One and a half years later (December 2022), even though cleaning up and rebuilding made progress, there are still marks of fine sediment in the affected areas. In the pavement joints as well as on rough walls, sediments are still trapped in the low-lying parts. Every brushing of these pavements will release some of the material. Regarding the broad deposition of fine sediments enriched in possibly toxic trace metal beyond critical threshold concentrations, there is a significant risk for the people exposed to the flood sediments in Eschweiler. Moreover, there is no level of PM exposure at which no health risk is to be expected [63].

The devastating character of the event led to a broad response in society with a high willingness to support as volunteers. In addition, the police, fire department, technical relief organization, the German Federal Armed Forces, medical specialists, and many other organizations were involved in the work with a high level of deployment [92, 97]. Thereby, not only those directly affected by the flooding are at risk, but everyone who contributed to the rescue, relief, and clean-up efforts. Even at the beginning of 2022, volunteers were still working in flood-affected regions [97].

This risk is also increased if the contaminated sediments come into contact with vulnerable groups of people. For example, children have a generally higher risk when exposed to trace metals [19, 121]. In a broader sense, vulnerability has frequently been shown to be related to several factors like demographics, health, socioeconomic factors, and risk perception [52, 90]. The 2021 July flood disproportionately affected vulnerable groups of people [9]. In the study area, kindergartens, schools, a retirement home, and a hospital were flooded, and thus contaminated sediments were also carried into these buildings.

Limitations due to unknown bioaccessibility

Bioaccessibility describes that part of any substance soluble in the target organ [120]. Hence, following ingestion, it is the gastrointestinal tract where gastric bioaccessibility plays the decisive role, while after inhalation, the respiratory bioaccessibility in the lungs is crucial. These two values can differ significantly [120]. Bioaccessibility depends on a complex interplay of physical and chemical properties of the element, like aggregation, binding to clay minerals, being part of a solid mineral structure, and many more. The preferred determination methods are extraction experiments (commonly used are Artificial lysosomal fluid or Gamble's solution; for details, see [61] and [69]), which is beyond the scope of this paper. Therefore, trace metal concentrations in this paper provide an upper-end estimate of potential toxicity [45]. General predictions on bioaccessibility are impossible, as the share available for uptake in the lungs varies greatly [81]; da Silva et al. [152] found values from 1.1% up to 93% to be bioaccessible. Yet, Luo et al. [122] found significant correlations between trace metal concentrations and human bioaccessibility. For the Inde catchment, a correlation between total trace metal concentrations and the generally bioaccessible fraction is proven [153].

Soluble metals are the main driver of the toxic potential of PM [61] as they can directly diffuse across the lung membrane [63]. High solubilities were proven for Pb, Cu, Cd, As, Sb, Sn, and Ni, which are enriched in the Eschweiler flood sediments [81, 120, 154]. Additionally, there is evidence that the melting process increases the bioaccessibility of metals (Cd and Pb) [120]. This is problematic, as much of the trace metals in the fluvial sediments of the Inde originate from mining legacies [102]. Furthermore, finer particles tend to have higher solubilities [75], which further enhances the risk of the inhalation of trace metal-enriched sediments.

Recommended actions

Considering the high chance of more frequent flooding in the future [3], the widespread deposition of fine flood sediments, and the persistence of trace metals in catchments influenced by former mining activities, we propose the following steps to address the exposure of the public to polluted high flood sediments:

I. Improving flood mapping

Numerical modeling proved to be a helpful tool to assess the areas affected by sediment deposition and might be useful as flood risk mapping needs to be improved to even smaller scales [93, 155]. However, the absolute sediment deposition might be overestimated due to the distinct features of cities, e.g., sewage systems. Flood maps should also include potential pollution sources like legacy

sites and industrial areas relevant to pollution so that it becomes visible where protection measurements are necessary and to warn people downstream who might be affected by the polluted sediments. However, in catchments affected by diffuse pollution, like the Inde catchment, it seems more appropriate to educate people about the pollution risks generally. Our results showed that all flood sediment samples were severely enriched in several risk elements and should therefore be treated cautiously.

II. Extending warning mechanisms

In the subsequent evaluation of the flooding event, it became apparent that warnings and awareness within the general public of flood-related risks were very much insufficient [88, 156]. Part of the problem was that the July 2021 flood exceeded all floods the affected people had experienced so far. Therefore, their safety measurements, which had proven reliable during other flood events, were insufficient [156]. Warning messages that include precise information on appropriate behavior significantly positively influence the ability to cope with the situation [157]. However, recommendations on behavior are sparse, with only one-third of media coverage in advance of the July flood dealing with it [157].

III. Improving clean-up activities

Dust clean-up is a difficult, often failed task [150] and should not rely only on purely mechanical methods as they often miss smaller particles [158]. Water flushing can be an effective tool to remove erodible sediments, reduce dust emissions and thereby prevent people's exposure to them [158]. Furthermore, post-flood cleaning has proven efficient in preventing indoor aerosol contamination [8].

IV. Specialized medical support

Thorough control of exposure to airborne particles, education about symptoms, and routine medical assessment build the best approach to prevent health issues [64]. People returning to their homes should be under the care of medical professionals [51]. The options for remediating in the Inde catchment are limited as a high input of diffuse sources has to be expected [159]. Therefore, protecting the endpoint, i.e., people, is the essential tool for mitigation. Educating people in advance instead of solely relying on warnings as soon as the event is predicted or even during it is a key point.

V. Raising awareness

Raising public awareness of the risks due to contaminated flood sediments, as well as educating about suitable safety measurements, is vital because the changes within the landscape due to the July 2021 flood may lead to a modified yet unpredictable response to smaller rainfall events in the future [90, 96]. The intense erosion led to the mobilization of large amounts of fine sediments that can now easily be eroded by smaller events, which consequently will have higher sediment loads [88]. Moreover, a decrease in the return period of similar events is projected by climate models [85, 86, 90], making the reduction of vulnerability and exposure a key task [90].

Conclusions

This study showed that during the extreme flooding of July 2021, large parts of the city of Eschweiler were covered with fine sediments enriched in possibly health-relevant trace metals. These sediments consist largely of fine material (32% to 96% < 63 µm), which can be easily entrained into the atmosphere and get inhaled, or they stick to the human skin, from where they can be ingested inadvertently. With regard to a potentially health-relevant intake of trace metals, only the concentrations of Pb appear to be of concern. However, other substances such as Zn, Cd, As, and Cu also exceed international concentration limits for sediments in most flood sediment samples. Therefore, long-term monitoring must be considered, also covering the effects on ecosystems. In addition, the effects of other pollutants, such as organic pollutants, mold, and fungi, which grow quickly in moist materials, pathogens, and mental health issues due to the traumatic experiences during the flood event, should be taken into account.

To address the health risks due to flood sediments, we propose to improve flood mapping, extend warning mechanisms to include guidance on appropriate behavior, and raise awareness for the health-related possible risks of flood sediments. In addition, in the aftermath of events like the July 2021 flooding, clean-up activities need to be improved to minimize dust generation, and people exposed to flood sediments, which also covers helpers, need to be provided with specialized medical support.

Abbreviations

EF	Enrichment factor
I_{geo}	Geoaccumulation index
JECFA	Joint FAO/WHO Expert Committee on Food Additives
PM	Particulate matter
PM_{50}	Particulate matter of < 50 µm diameter
PM_{10}	Particulate matter of < 10 µm diameter
$PM_{2.5}$	Particulate matter of < 2.5 µm diameter
PTDI	Probable tolerable daily intake
XRF	X-ray fluorescence

Acknowledgements

We thank Verena Esser, Philipp Schulte, Eva Vonden, Fabian Weichert, Klaus Reicherter, and Janine Freyer for their help with collecting samples. We thank

Verena Esser for helping with sorting and cataloging the samples. We thank Marianne Dohms and Renate Erdweg for the laboratory analysis. We thank Janine Freyer for measuring flood marks and Lennart Schelter and Jaron Auracher for digitizing them. Helpful comments by Jan Schwarzbauer and an anonymous reviewer are highly appreciated. We owe a great debt of gratitude to the ABC/J Geoverbund, who financially supports the work of the HyCo-Geo Competence Centre. Furthermore, we acknowledge the financial support by the Deutsche Forschungsgemeinschaft and the Robust Nature Excellence Initiative at Goethe University Frankfurt.

Author contributions
Conceptualization, AW; methodology, AW, SW, NB; sampling, SW, PB, EK; data analysis, AW; numerical modeling, SW, LMN; writing—original draft preparation, AW, SW; writing—review and editing, AW, SW, PB, FL; visualization, AW and SW; supervision, CB, FL; project administration, CB, FL, HS, HH; funding acquisition, CB, FL and HS. All authors read and approved the final manuscript.

Funding
Open Access funding enabled and organized by Projekt DEAL. This work is supported by the Deutsche Forschungsgemeinschaft (DFG) under project numbers 496274914 and 497800446 and the RobustNature Excellence Initiative at Goethe University Frankfurt. This work has been developed within the framework of the competence center HyCo-Geo funded by the ABC/J Geoverbund.

Availability of data and materials
The datasets used and analyzed during the current study are available from the corresponding author upon reasonable request.

Declarations

Ethics approval and consent to participate
Not applicable.

Consent for publication
Not applicable.

Competing interests
The authors declare that they have no competing interests.

Author details
[1]Department of Geography, RWTH Aachen University, Wüllnerstr. 5B, 52062 Aachen, Germany. [2]Institute of Hydraulic Engineering and Water Resources Management, RWTH Aachen University, Mies-van-der-Rohe-Straße 17, 52056 Aachen, Germany. [3]Department Evolutionary Ecology & Environmental Toxicology (E3T), Faculty Biological Sciences (FB15), Goethe University Frankfurt, Max-Von-Laue-Str. 13, 60438 Frankfurt am Main, Germany. [4]Institute of Neotectonics and Natural Hazards, RWTH Aachen University, Lochnerstrasse 4-20, 52056 Aachen, Germany. [5]Department Environmental Media Related Ecotoxicology, Fraunhofer Institute for Molecular Biology and Applied Ecology IME, 57392 Schmallenberg, Germany. [6]LOEWE Centre for Translational Biodiversity Genomics (LOEWE-TBG), Senckenberganlage 25, 60325 Frankfurt am Main, Germany.

Received: 3 March 2023 Accepted: 18 July 2023
Published online: 28 July 2023

References

1. Milly PCD, Wetherald RT, Dunne KA, Delworth TL (2002) Increasing risk of great floods in a changing climate. Nature 415:514–517. https://doi.org/10.1038/415514a
2. Bell JE, Brown CL, Conlon K, Herring S, Kunkel KE, Lawrimore J et al (2018) Changes in extreme events and the potential impacts on human health. J Air Waste Manag Assoc 68:265–287. https://doi.org/10.1080/10962247.2017.1401017
3. Blöschl G, Hall J, Viglione A, Perdigão RAP, Parajka J, Merz B et al (2019) Changing climate both increases and decreases European river floods. Nature 573:108–111. https://doi.org/10.1038/s41586-019-1495-6
4. Foulds SA, Brewer PA, Macklin MG, Haresign W, Betson RE, Rassner SME (2014) Flood-related contamination in catchments affected by historical metal mining: an unexpected and emerging hazard of climate change. Sci Total Environ 476–477:165–180. https://doi.org/10.1016/j.scitotenv.2013.12.079
5. Coynel A, Schäfer J, Blanc G, Bossy C (2007) Scenario of particulate trace metal and metalloid transport during a major flood event inferred from transient geochemical signals. Appl Geochem 22:821–836. https://doi.org/10.1016/j.apgeochem.2006.10.004
6. Resongles E, Casiot C, Freydier R, Le Gall M, Elbaz-Poulichet F (2015) Variation of dissolved and particulate metal(loid) (As, Cd, Pb, Sb, Tl, Zn) concentrations under varying discharge during a Mediterranean flood in a former mining watershed, the Gardon River (France). J Geochem Explor 158:132–142. https://doi.org/10.1016/j.gexplo.2015.07.010
7. Crawford SE, Brinkmann M, Ouellet JD, Lehmkuhl F, Reicherter K, Schwarzbauer J et al (2022) Remobilization of pollutants during extreme flood events poses severe risks to human and environmental health. J Hazard Mater 421:126691. https://doi.org/10.1016/j.jhazmat.2021.126691
8. He C, Salonen H, Ling X, Crilley L, Jayasundara N, Cheung HC et al (2014) The impact of flood and post-flood cleaning on airborne microbiological and particle contamination in residential houses. Environ Int 69:9–17. https://doi.org/10.1016/j.envint.2014.04.001
9. Lehmkuhl F, Schüttrumpf H, Schwarzbauer J, Brüll C, Dietze M, Letmathe P et al (2022) Assessment of the 2021 summer flood in Central Europe. Environ Sci Eur. https://doi.org/10.1186/s12302-022-00685-1
10. Förstner U (2004) Sediment dynamics and pollutant mobility in rivers: an interdisciplinary approach. Lakes Reserv 9:25–40. https://doi.org/10.1111/j.1440-1770.2004.00231.x
11. Ciszewski D, Grygar TM (2016) A review of flood-related storage and remobilization of heavy metal pollutants in river systems. Water Air Soil Pollut 227:239. https://doi.org/10.1007/s11270-016-2934-8
12. Špitalar M, Gourley JJ, Lutoff C, Kirstetter P-E, Brilly M, Carr N (2014) Analysis of flash flood parameters and human impacts in the US from 2006 to 2012. J Hydrol 519:863–870. https://doi.org/10.1016/j.jhydrol.2014.07.004
13. Bronstert A, Crisologo I, Heistermann M, Ozturk U, Vogel K, Wendi D (2020) Flash-floods: more often, more severe, more damaging? An analysis of hydro-geo-environmental conditions and anthropogenic impacts. In: Leal Filho W, Nagy GJ, Borga M, Chávez Muñoz PD, Magnuszewski A (eds) Climate change, hazards and adaptation options. Springer International Publishing, Cham, pp 225–244. https://doi.org/10.1007/978-3-030-37425-9_12
14. Gems B, Mazzorana B, Hofer T, Sturm M, Gabl R, Aufleger M (2016) 3-D hydrodynamic modelling of flood impacts on a building and indoor flooding processes. Nat Hazards Earth Syst Sci 16:1351–1368. https://doi.org/10.5194/nhess-16-1351-2016
15. Macklin MG, Brewer PA, Hudson-Edwards KA, Bird G, Coulthard TJ, Dennis IA et al (2006) A geomorphological approach to the management of rivers contaminated by metal mining. Geomorphology 79:423–447. https://doi.org/10.1016/j.geomorph.2006.06.024
16. Förstner U, Müller G (1973) Heavy metal accumulation in river sediments: a response to environmental pollution. Geoforum 4:53–61. https://doi.org/10.1016/0016-7185(73)90006-7
17. Albering HJ, van Leusen SM, Moonen EJ, Hoogewerff JA, Kleinjans JC (1999) Human health risk assessment: a case study involving heavy metal soil contamination after the flooding of the river Meuse during the winter of 1993–1994. Environ Health Perspect 107:37–43. https://doi.org/10.1289/ehp.9910737
18. Coulthard TJ, Macklin MG (2003) Modeling long-term contamination in river systems from historical metal mining. Geology 31:451. https://doi.org/10.1130/0091-7613(2003)031%3C0451:MLCIRS%3E2.0.CO;2
19. Bundschuh J, Schneider J, Alam MA, Niazi NK, Herath I, Parvez F et al (2021) Seven potential sources of arsenic pollution in Latin America and their environmental and health impacts. Sci Total Environ 780:146274. https://doi.org/10.1016/j.scitotenv.2021.146274
20. Resongles E, Casiot C, Freydier R, Dezileau L, Viers J, Elbaz-Poulichet F (2014) Persisting impact of historical mining activity to metal (Pb, Zn, Cd, Tl, Hg) and metalloid (As, Sb) enrichment in sediments of the Gardon River, Southern France. Sci Total Environ 481:509–521. https://doi.org/10.1016/j.scitotenv.2014.02.078

21. Axtmann EV, Luoma SN (1991) Large-scale distribution of metal contamination in the fine-grained sediments of the Clark Fork River, Montana, U.S.A. Appl Geochem 6:75–88. https://doi.org/10.1016/0883-2927(91)90064-V
22. Byrne P, Reid I, Wood PJ (2013) Stormflow hydrochemistry of a river draining an abandoned metal mine: the Afon Twymyn, central Wales. Environ Monit Assess 185:2817–2832. https://doi.org/10.1007/s10661-012-2751-5
23. Cánovas CR, Olías M, Sarmiento AM, Nieto JM, Galván L (2012) Pollutant transport processes in the Odiel River (SW Spain) during rain events. Water Resour Res. https://doi.org/10.1029/2011WR011041
24. Ciszewski D (2001) Flood-related changes in heavy metal concentrations within sediments of the Biaa Przemsza River. Geomorphology 40:205–218. https://doi.org/10.1016/S0169-555X(01)00044-7
25. Dawson EJ, Macklin MG (1998) Speciation of heavy metals on suspended sediment under high flow conditions in the River Aire, West Yorkshire. UK Hydrol Process 12:1483–1494. https://doi.org/10.1002/(SICI)1099-1085(199807)12:9%3C1483::AID-HYP651%3E3.0.CO;2-W
26. Miller J, Barr R, Grow D, Lechler P, Richardson D, Waltman K, Warwick J (1999) Effects of the 1997 flood on the transport and storage of sediment and mercury within the Carson River Valley, West-Central Nevada. J Geol 107:313–327. https://doi.org/10.1086/314353
27. Strzebońska M, Kostka A, Helios-Rybicka E, Jarosz-Krzemińska E (2015) Effect of flooding on heavy metals contamination of Vistula floodplain sediments in cracow; historical mining and smelting as the most important source of pollution. Pol J Environ Stud 24:1317–1326. https://doi.org/10.15244/pjoes/33202
28. Žák K, Rohovec J, Navrátil T (2009) Fluxes of heavy metals from a highly polluted watershed during flood events: a case study of the Litavka River, Czech Republic. Water Air Soil Pollut 203:343–358. https://doi.org/10.1007/s11270-009-0017-9
29. Martin CW (2015) Trace metal storage in recent floodplain sediments along the Dill River, central Germany. Geomorphology 235:52–62. https://doi.org/10.1016/j.geomorph.2015.01.032
30. Hürkamp K, Raab T, Völkel J (2009) Lead pollution of floodplain soils in a historic mining area—age, distribution and binding forms. Water Air Soil Pollut 201:331–345. https://doi.org/10.1007/s11270-008-9948-9
31. Ponting J, Kelly TJ, Verhoef A, Watts MJ, Sizmur T (2021) The impact of increased flooding occurrence on the mobility of potentially toxic elements in floodplain soil—a review. Sci Total Environ 754:142040. https://doi.org/10.1016/j.scitotenv.2020.142040
32. Dennis IA, Macklin MG, Coulthard TJ, Brewer PA (2003) The impact of the October–November 2000 floods on contaminant metal dispersal in the River Swale catchment, North Yorkshire. UK Hydrol Process 17:1641–1657. https://doi.org/10.1002/hyp.1206
33. Sauvé S, Hendershot W, Allen HE (2000) Solid-solution partitioning of metals in contaminated soils: dependence on pH, total metal burden, and organic matter. Environ Sci Technol 34:1125–1131. https://doi.org/10.1021/es9907764
34. Miller JR (1997) The role of fluvial geomorphic processes in the dispersal of heavy metals from mine sites. J Geochem Explor 58:101–118. https://doi.org/10.1016/S0375-6742(96)00073-8
35. Chen J-B, Gaillardet J, Bouchez J, Louvat P, Wang Y-N (2014) Anthropophile elements in river sediments: Overview from the Seine River, France. Geochem Geophys Geosyst 15:4526–4546. https://doi.org/10.1002/2014GC005516
36. Foster IDL, Charlesworth SM (1996) Heavy metals in the hydrological cycle: trends and explanation. Hydrol Process 10:227–261. https://doi.org/10.1002/(SICI)1099-1085(199602)10:2%3C227::AID-HYP357%3E3.0.CO;2-X
37. Navrátil T, Rohovec J, Žák K (2008) Floodplain sediments of the 2002 catastrophic flood at the Vltava (Moldau) River and its tributaries: mineralogy, chemical composition, and post-sedimentary evolution. Environ Geol 56:399–412. https://doi.org/10.1007/s00254-007-1178-8
38. Bradley SB, Lewin J (1982) Transport of heavy metals on suspended sediments under high flow conditions in a mineralised region of wales. Environ Pollut B 4:257–267. https://doi.org/10.1016/0143-148X(82)90012-X
39. Bradley SB (1984) Flood effects on the transport of heavy metals. Int J Environ Stud 22:225–230. https://doi.org/10.1080/00207238408710121
40. Pulley S, Foster I, Antunes P (2016) The dynamics of sediment-associated contaminants over a transition from drought to multiple flood events in a lowland UK catchment. Hydrol Process 30:704–719. https://doi.org/10.1002/hyp.10616
41. Derbyshire E (2013) Natural aerosolic mineral dusts and human health. In: Selinus O (ed) Essentials of medical geology. Springer Netherlands, Dordrecht, pp 455–475. https://doi.org/10.1007/978-94-007-4375-5_19
42. Kok JF, Parteli EJR, Michaels TI, Karam DB (2012) The physics of wind-blown sand and dust. Rep Prog Phys 75:106901. https://doi.org/10.1088/0034-4885/75/10/106901
43. Derbyshire E (2007) Natural minerogenic dust and human health. AMBIO: J Hum Environ 36:73–77. https://doi.org/10.1579/0044-7447(2007)36[73:NMDAHH]2.0.CO;2
44. Pye K (1987) Aeolian dust and dust deposits. Elsevier, Amsterdam
45. Mukhtar A, Limbeck A (2013) Recent developments in assessment of bio-accessible trace metal fractions in airborne particulate matter: a review. Anal Chim Acta 774:11–25. https://doi.org/10.1016/j.aca.2013.02.008
46. Újvári G, Kok JF, Varga G, Kovács J (2016) The physics of wind-blown loess: implications for grain size proxy interpretations in quaternary paleoclimate studies. Earth Sci Rev 154:247–278. https://doi.org/10.1016/j.earscirev.2016.01.006
47. Bloom E, Grimsley LF, Pehrson C, Lewis J, Larsson L (2009) Molds and mycotoxins in dust from water-damaged homes in New Orleans after hurricane Katrina. Indoor Air 19:153–158. https://doi.org/10.1111/j.1600-0668.2008.00574.x
48. Ashley NA, Valsaraj KT, Thibodeaux LJ (2008) Elevated in-home sediment contaminant concentrations—the consequence of a particle settling-winnowing process from Hurricane Katrina floodwaters. Chemosphere 70:833–840. https://doi.org/10.1016/j.chemosphere.2007.07.010
49. Presley SM, Rainwater TR, Austin GP, Platt SG, Zak JC, Cobb GP et al (2006) Assessment of pathogens and toxicants in New Orleans, LA following Hurricane Katrina. Environ Sci Technol 40:468–474. https://doi.org/10.1021/es052219p
50. Wang K, You D, Balakrishna S, Ripple M, Ahlert T, Fahmy B et al (2008) Sediment from Hurricane Katrina: potential to produce pulmonary dysfunction in mice. Int J Clin Exp Med 1:130–144
51. Hoppe KA, Metwali N, Perry SS, Hart T, Kostle PA, Thorne PS (2012) Assessment of airborne exposures and health in flooded homes undergoing renovation. Indoor Air 22:446–456. https://doi.org/10.1111/j.1600-0668.2012.00785.x
52. Davidson CI, Phalen RF, Solomon PA (2005) Airborne particulate matter and human health: a review. Aerosol Sci Technol 39:737–749. https://doi.org/10.1080/02786820500191348
53. Schwartz J (1994) Air pollution and daily mortality: a review and meta analysis. Environ Res 64:36–52. https://doi.org/10.1006/enrs.1994.1005
54. Tranfield E, Walker D (2012) Understanding human illness and death following exposure to particulate matter air pollution. In: Oosthuizen J (ed) Environmental health—emerging issues and practice. Rijeka, InTech, pp 82–102
55. Pope CA, Schwartz J, Ransom MR (1992) Daily mortality and PM10 pollution in Utah Valley. Arch Environ Health 47:211–217. https://doi.org/10.1080/00039896.1992.9938351
56. Kim SE, Bell ML, Hashizume M, Honda Y, Kan H, Kim H (2018) Associations between mortality and prolonged exposure to elevated particulate matter concentrations in East Asia. Environ Int 110:88–94. https://doi.org/10.1016/j.envint.2017.10.010
57. Fairley D (1990) The relationship of daily mortality to suspended particulates in Santa Clara County, 1980–1986. Environ Health Perspect 89:159. https://doi.org/10.2307/3430912
58. Schwartz J, Dockery DW (1992) Increased mortality in Philadelphia associated with daily air pollution concentrations. Am Rev Respir Dis 145:600–604. https://doi.org/10.1164/ajrccm/145.3.600
59. Morman SA, Plumlee GS (2013) The role of airborne mineral dusts in human disease. Aeol Res 9:203–212. https://doi.org/10.1016/j.aeolia.2012.12.001
60. Liu X, Nie D, Zhang K, Wang Z, Li X, Shi Z et al (2019) Evaluation of particulate matter deposition in the human respiratory tract during winter in Nanjing using size and chemically resolved ambient

measurements. Air Qual Atmos Health 12:529–538. https://doi.org/10.1007/s11869-019-00663-2
61. Wiseman CLS (2015) Analytical methods for assessing metal bioaccessibility in airborne particulate matter: a scoping review. Anal Chim Acta 877:9–18. https://doi.org/10.1016/j.aca.2015.01.024
62. Gioda A, Peréz U, Rosa Z, Jimenez-Velez B (2007) Particulate matter (PM10 and PM2.5) from different areas of Puerto Rico. Fresenius Environ Bull 16:861–868
63. Cassee FR, Héroux M-E, Gerlofs-Nijland ME, Kelly FJ (2013) Particulate matter beyond mass: recent health evidence on the role of fractions, chemical constituents and sources of emission. Inhal Toxicol 25:802–812. https://doi.org/10.3109/08958378.2013.850127
64. Leung CC, Yu ITS, Chen W (2012) Silicosis. The Lancet 379:2008–2018. https://doi.org/10.1016/S0140-6736(12)60235-9
65. Barnes H, Goh NSL, Leong TL, Hoy R (2019) Silica-associated lung disease: an old-world exposure in modern industries. Respirology 24:1165–1175. https://doi.org/10.1111/resp.13695
66. Leetham M, DeWitt J, Buck B, Goossens D, Teng Y, Pollard J et al (2016) Oxidative stress and lung pathology following geogenic dust exposure. J Appl Toxicol 36:1276–1283. https://doi.org/10.1002/jat.3297
67. Knaapen AM, Shi T, Borm PJ, Schins RP (2002) Soluble metals as well as the insoluble particle fraction are involved in cellular DNA damage induced by particulate matter. Mol Cell Biochem 234(235):317–326. https://doi.org/10.1023/A:1015970023889
68. Dominici F, Peng RD, Ebisu K, Zeger SL, Samet JM, Bell ML (2007) Does the effect of PM10 on mortality depend on PM nickel and vanadium content? A reanalysis of the NMMAPS data. Environ Health Perspect 115:1701–1703. https://doi.org/10.1289/ehp.10737
69. Kastury F, Smith E, Juhasz AL (2017) A critical review of approaches and limitations of inhalation bioavailability and bioaccessibility of metal(loid)s from ambient particulate matter or dust. Sci Total Environ 574:1054–1074. https://doi.org/10.1016/j.scitotenv.2016.09.056
70. Laidlaw M, Filippelli G (2008) Resuspension of urban soils as a persistent source of lead poisoning in children: a review and new directions. Appl Geochem 23:2021–2039
71. Bi X, Li Z, Sun G, Liu J, Han Z (2015) In vitro bioaccessibility of lead in surface dust and implications for human exposure: a comparative study between industrial area and urban district. J Hazard Mater 297:191–197. https://doi.org/10.1016/j.jhazmat.2015.04.074
72. Costa DL, Dreher KL (1997) Bioavailable transition metals in particulate matter mediate cardiopulmonary injury in healthy and compromised animal models. Environ Health Perspect 105:1053. https://doi.org/10.2307/3433509
73. Belliardo C, Di Giorgio C, Chaspoul F, Gallice P, Bergé-Lefranc D (2018) Direct DNA interaction and genotoxic impact of three metals: cadmium, nickel and aluminum. J Chem Thermodyn 125:271–277. https://doi.org/10.1016/j.jct.2018.05.028
74. Gagnon ZE, Newkirk C, Hicks S (2006) Impact of platinum group metals on the environment: a toxicological, genotoxic and analytical chemistry study. J Environ Sci Health A Tox Hazard Subst Environ Eng 41:397–414. https://doi.org/10.1080/10934520500423592
75. Mason LH, Harp JP, Han DY (2014) Pb neurotoxicity: neuropsychological effects of lead toxicity. Biomed Res Int 2014:840547. https://doi.org/10.1155/2014/840547
76. Pritchard RJ, Ghio AJ, Lehmann JR, Winsett DW, Tepper JS, Park P et al (1996) Oxidant generation and lung injury after particulate air pollutant exposure increase with the concentrations of associated metals. Inhal Toxicol 8:457–477. https://doi.org/10.3109/08958379609005440
77. Kasprzak KS (2002) Oxidative DNA and protein damage in metal-induced toxicity and carcinogenesis. Free Radic Biol Med 32:958–967. https://doi.org/10.1016/S0891-5849(02)00809-2
78. Valavanidis A (2000) Generation of hydroxyl radicals by urban suspended particulate air matter. The role of iron ions. Atmos Environ 34:2379–2386. https://doi.org/10.1016/S1352-2310(99)00435-5
79. Schaumann F, Borm PJA, Herbrich A, Knoch J, Pitz M, Schins RPF et al (2004) Metal-rich ambient particles (particulate matter 2.5) cause airway inflammation in healthy subjects. Am J Respir Crit Care Med 170:898–903. https://doi.org/10.1164/rccm.200403-423OC
80. Peters S, Reid A, Fritschi L, de Klerk N, Musk AWB (2013) Long-term effects of aluminium dust inhalation. Occup Environ Med 70:864–868. https://doi.org/10.1136/oemed-2013-101487
81. Wiseman CL, Zereini F (2014) Characterizing metal(loid) solubility in airborne PM10, PM2.5 and PM1 in Frankfurt, Germany using simulated lung fluids. Atmos Environ 89:282–289. https://doi.org/10.1016/j.atmosenv.2014.02.055
82. Pohl HR, Roney N, Abadin HG (2011) Metal ions affecting the neurological system. Met Ions Life Sci 8:247–262
83. Cook A, Derbyshire E, Plumlee G (2011) Impact of natural dusts on human health. In: Encyclopedia of environmental health. Elsevier, p 178–186. https://doi.org/10.1016/B978-0-444-52272-6.00162-8
84. meinstolberg.de (22.07.2021) Masken wegen hoher Staubbelastung mit Schadstoffen empfohlen
85. Belleflamme A, Goergen K, Iakunin M, Vanderborght J, Kollet S (2021) The extreme flood events of summer 2021 in western Germany and Belgium as simulated by the free-running ParFlow hydrological model
86. Junghänel T, Bissolli P, Daßler J, Fleckenstein R, Imbery F, Janssen W, et al (2021) Hydro-klimatische Einordnung der Stark- und Dauerniederschläge in Teilen Deutschlands im Zusammenhang mit dem Tiefdruckgebiet „Bernd" vom 12. bis 19. Juli 2021.
87. Schäfer A, Mühr B, Daniell J, Ehret U, Ehmele F, Küpfer K, et al (2021) Hochwasser Mitteleuropa, Juli 2021 (Deutschland) : 21. Juli 2021 – Bericht Nr. 1 „Nordrhein-Westfalen & Rheinland-Pfalz". Karlsruher Institut für Technologie (KIT)
88. Dietze M, Bell R, Ozturk U, Cook KL, Andermann C, Beer AR et al (2022) More than heavy rain turning into fast-flowing water—a landscape perspective on the 2021 Eifel floods. Nat Hazards Earth Syst Sci 22:1845–1856. https://doi.org/10.5194/nhess-22-1845-2022
89. Meyer W (2013) Geologie der Eifel: Mit 12 Tabellen, 4th edn. Schweizerbart, Stuttgart
90. Kreienkamp F, Philip SY, Tradowsky JS, Kew SF, Lorenz P, Arrighi J, et al. Rapid attribution of heavy rainfall events leading to the severe flooding in Western Europe during July 2021
91. Marchi L, Borga M, Preciso E, Gaume E (2010) Characterisation of selected extreme flash floods in Europe and implications for flood risk management. J Hydrol 394:118–133. https://doi.org/10.1016/j.jhydrol.2010.07.017
92. Bundesministerium des Inneren, für Bau und Heimat, Bundesministerium der Finanzen (2022) Bericht zur Hochwasserkatastrophe 2021: Katastrophenhilfe, Wiederaufbau und Evaluierungsprozesse
93. Dietze M, Ozturk U (2021) A flood of disaster response challenges. Science 373:1317–1318. https://doi.org/10.1126/science.abm0617
94. Dietze M, Hoffmann T, Bell R, Schrott L, Hovius N (2022) A seismic approach to flood detection and characterization in upland catchments. Geophys Res Lett. https://doi.org/10.1029/2022GL100170
95. Mohr S, Ehret U, Kunz M, Ludwig P, Caldas-Alvarez A, Daniell JE et al (2023) A multi-disciplinary analysis of the exceptional flood event of July 2021 in central Europe—part 1: event description and analysis. Nat Hazards Earth Syst Sci 23:525–551. https://doi.org/10.5194/nhess-23-525-2023
96. Bell R, Dietze M, Thieken A, Cook K, Andermann C, Beer A, et al (2022) More than just fast flowing water: the landscape impact of the July 2021 west Germany flood
97. Bell R, Kron W, Thiebes B, Thieken A (2022) Die Flutkatastrophe im Juli 2021: Ein Jahr danach: Aufarbeitung und erste Lehren für die Zukunft, Bonn
98. Koks E, van Ginkel K, van Marle M, Lemnitzer A (2021) Brief communication: Critical Infrastructure impacts of the 2021 mid-July western European flood event. Nat Hazard Earth Syst Sci Discuss. https://doi.org/10.5194/nhess-2021-394
99. Geologischer Dienst NRW (2016) Geologische Detaildarstellung: Blatt L 5102 Geilenkirchen. Geologischer Dienst NRW, Krefeld
100. Geologischer Dienst NRW (2016) Geologische Detaildarstellung: Blatt L 5302 Aachen. Geologischer Dienst NRW, Krefeld
101. Bosselmann H (2008) Indeausbau und Hochwasserschutz in den Jahren 1960–1992. Schriftenreihe des Eschweiler Geschichtsvereins 25:41–48
102. Esser V, Buchty-Lemke M, Schulte P, Podzun LS, Lehmkuhl F (2020) Signatures of recent pollution profiles in comparable central European rivers—examples from the international River Basin District Meuse. CATENA 193:104646. https://doi.org/10.1016/j.catena.2020.104646
103. Esser V (2020) Investigations on fluvial morphodynamics and recent pollutant dispersion in river systems—examples from the border

region of Belgium, the Netherlands and Germany. Dissertation, RWTH Aachen University, Aachen
104. MKULNV NRW (2014) Maas Süd. Steckbriefe der planungseinheiten in den Nordrhein-westfälischen Anteilen von Rhein, Weser, Ems und Maas: Oberflächengewässer und Grundwasser Teileinzugsgebiet Maas/Maas Süd NRW, Düsseldorf
105. Schulte P, Lehmkuhl F, Steininger F, Loibl D, Lockot G, Protze J et al (2016) Influence of HCl pretreatment and organo-mineral complexes on laser diffraction measurement of loess–paleosol-sequences. CATENA 137:392–405. https://doi.org/10.1016/j.catena.2015.10.015
106. Blott SJ, Pye K (2001) GRADISTAT: a grain size distribution and statistics package for the analysis of unconsolidated sediments. Earth Surf Process Landf 26:1237–1248. https://doi.org/10.1002/esp.261
107. DIN ISO 11277 Soil quality: determination of particle size distribution in mineral soil material—method by sieving and sedimentation 2002
108. Özer M, Orhan M, Isik NS (2010) Effect of particle optical properties on size distribution of soils obtained by laser diffraction. Environ Eng Geosci 16:163–173. https://doi.org/10.2113/gseegeosci.16.2.163
109. ISO 13320 Particle size analysis—laser diffraction methods: part 1: general principles, Annex A: theoretical background of laser diffraction 2009
110. Bábek O, Grygar TM, Faměra M, Hron K, Nováková T, Sedláček J (2015) Geochemical background in polluted river sediments: how to separate the effects of sediment provenance and grain size with statistical rigour? CATENA 135:240–253. https://doi.org/10.1016/j.catena.2015.07.003
111. SPECTRO (2007) Analysis of trace elements in geological materials, soils and sludges prepared as pressed pellets
112. Amorosi A, Guermandi M, Marchi N, Sammartino I (2014) Fingerprinting sedimentary and soil units by their natural metal contents: a new approach to assess metal contamination. Sci Total Environ 500–501:361–372. https://doi.org/10.1016/j.scitotenv.2014.08.078
113. Ersoy A (2021) Critical review of the environmental investigation on soil heavy metal contamination. Appl Ecol Env Res 19:3853–3878. https://doi.org/10.15666/aeer/1905_38533878
114. Matys Grygar T, Popelka J (2016) Revisiting geochemical methods of distinguishing natural concentrations and pollution by risk elements in fluvial sediments. J Geochem Explor 170:39–57. https://doi.org/10.1016/j.gexplo.2016.08.003
115. Bábek O, Faměra M, Hilscherová K, Kalvoda J, Dobrovolný P, Sedláček J et al (2011) Geochemical traces of flood layers in the fluvial sedimentary archive; implications for contamination history analyses. CATENA 87:281–290. https://doi.org/10.1016/j.catena.2011.06.014
116. Matschullat J, Ottenstein R, Reimann C (2000) Geochemical background—can we calculate it? Environ Geol 39:990–1000. https://doi.org/10.1007/s002549900084
117. Newman BK, Watling RJ (2019) Definition of baseline metal concentrations for assessing metal enrichment of sediment from the southeastern Cape coastline of South Africa. WSA. https://doi.org/10.4314/wsa.v33i5.184089
118. Müller G (1986) Schadstoffe in Sedimenten - Sedimente als Schadstoffe. Mitt Österr Geol Ges 79:107–126
119. U.S. EPA (2017) Update for Chapter 5 of the exposure factors handbook: soil and dust ingestion, Washington (DC)
120. Goix S, Uzu G, Oliva P, Barraza F, Calas A, Castet S et al (2016) Metal concentration and bioaccessibility in different particle sizes of dust and aerosols to refine metal exposure assessment. J Hazard Mater 317:552–562. https://doi.org/10.1016/j.jhazmat.2016.05.083
121. Rinklebe J, Antoniadis V, Shaheen SM, Rosche O, Altermann M (2019) Health risk assessment of potentially toxic elements in soils along the Central Elbe River, Germany. Environ Int 126:76–88. https://doi.org/10.1016/j.envint.2019.02.011
122. Luo X, Yu S, Li X (2011) Distribution, availability, and sources of trace metals in different particle size fractions of urban soils in Hong Kong: implications for assessing the risk to human health. Environ Pollut 159:1317–1326. https://doi.org/10.1016/j.envpol.2011.01.013
123. Bezirksregierung Köln (2019) Hachwassergefahrenkarte Inde: Kartenblatt 10/18. Land NRW
124. Bezirksregierung Köln (2019) Hochwassergefahrenkarte Inde (2824): Kartenblatt 8/18. Land NRW
125. Bezirksregierung Köln (2019) Hochwassergefahrenkarte Inde (2824): Kartenblatt 9/18. Land NRW
126. Cheng N-S (1997) Simplified settling velocity formula for sediment particle. J Hydraul Eng 123:149–152. https://doi.org/10.1061/(ASCE)0733-9429(1997)123:2(149)
127. Maaß A-L, Schüttrumpf H (2019) Reactivation of floodplains in river restorations: long-term implications on the mobility of floodplain sediment deposits. Water Resour Res 55:8178–8196. https://doi.org/10.1029/2019WR024983
128. Kabata-Pendias A (2010) Trace elements in soils and plants. CRC Press
129. US EPA (2003) Attachment 1–1: guidance for developing ecological soil screening levels (Eco-SSLs): review of existing soil screening benchmarks
130. Holtz F (2021) Glas in Stolberg. http://www.stolberg-abc.de/glas/glastxt.htm
131. WHO (2011) Safety evaluation of certain food additives and contaminants: Lead. World Health Organisation, Geneva
132. WHO (2011) Safety evaluation of certain food additives and contaminants: Arsenic. World Health Organisation, Geneva
133. WHO (2011) Safety evaluation of certain food additives and contaminants: Cadmium. World Health Organisation, Geneva
134. WHO (2003) Antimony in drinking-water: background document for development of who guidelines for drinking-water quality. World Health Organisation, Geneva
135. Schrenk D, Bignami M, Bodin L, Chipman JK, Del Mazo J, Grasl-Kraupp B et al (2020) Update of the risk assessment of nickel in food and drinking water. EFSA J 18:e06268. https://doi.org/10.2903/j.efsa.2020.6268
136. WHO (1982) Evaluation of certain food additives and contaminants: twenty-sixth report of the Joint FAO/WHO Extpert Committee of Food Additives, Geneva
137. WHO (2006) Safety evaluation of certain food additives and contaminants: Prepared by the sixty-fourth meeting of the Joint FAO/WHO Expert Committee on Food Additives (JECFA), Geneva
138. Stadt Stolberg (2023) Wirtschaftsstandort Stolberg: Die Kuperstadt Stolberg - Ein Industriestandort im Wandel. https://www.stolberg.de/city_info/webaccessibility/index.cfm?modul_id=5&record_id=681
139. Bayerisches Landesamt für Wasserwirtschaft (2000) Schwermetalle im kommunalen Abwasser und Klärschlamm, München
140. Landesamt für Natur, Umwelt und Verbraucherschutz Nordrhein-Westfalen (2018) Entwicklung und Stand der Abwasserbeseitigung in Nordrhein-Westfalen, Düsseldorf
141. Lehmkuhl F, Weber A, Esser V, Schulte P, Wolf S, Schrumpf H (2022) Fluviale Morphodynamik und Sedimentkontamination bei Extremereignissen: Das Juli-Hochwasser 2021 im Inde-Einzugsgebiet (Nordrhein-Westfalen). Korrespondenz Wasserwirtschaft, pp 422–427
142. Al-Ghafari A, Elmorsy E, Fikry E, Alrowaili M, Carter WG (2019) The heavy metals lead and cadmium are cytotoxic to human bone osteoblasts via induction of redox stress. PLoS ONE 14:e0225341. https://doi.org/10.1371/journal.pone.0225341
143. Laidlaw MA, Zahran S, Mielke HW, Taylor MP, Filippelli GM (2012) Resuspension of lead contaminated urban soil as a dominant source of atmospheric lead in Birmingham, Chicago, Detroit and Pittsburgh, USA. Atmos Environ 49:302–310. https://doi.org/10.1016/j.atmosenv.2011.11.030
144. Sweeney MR, Fischer B, Wermers K, Cowman T (2019) Eolian and fluvial modification of Missouri River sandbars deposited by the 2011 flood, USA. Geomorphology 327:111–125. https://doi.org/10.1016/j.geomorph.2018.10.018
145. Heal MR, Hibbs LR, Agius RM, Beverland IJ (2005) Total and water-soluble trace metal content of urban background PM10, PM2.5 and black smoke in Edinburgh. UK Atmos Environ 39:1417–1430. https://doi.org/10.1016/j.atmosenv.2004.11.026
146. Rasmussen PE, Levesque C, Chénier M, Gardner HD (2018) Contribution of metals in resuspended dust to indoor and personal inhalation exposures: relationships between PM10 and settled dust. Build Environ 143:513–522. https://doi.org/10.1016/j.buildenv.2018.07.044
147. Segalin B, Fornaro A, Kumar P, Klemm O, Andrade M, Trezza BM et al (2020) Chemical composition of quasi-ultrafine particles and their sources in elderly residences of São Paulo megacity. Aerosol Air Qual Res 20:1100–1015

148. Hunt A, Johnson DL, Griffith DA (2006) Mass transfer of soil indoors by track-in on footwear. Sci Total Environ 370:360–371. https://doi.org/10.1016/j.scitotenv.2006.07.013
149. Siciliano SD, James K, Zhang G, Schafer AN, Peak JD (2009) Adhesion and enrichment of metals on human hands from contaminated soil at an Arctic urban brownfield. Environ Sci Technol 43:6385–6390. https://doi.org/10.1021/es901090w
150. Choate LM, Ranville JF, Bunge AL, Macalady DL (2006) Dermally adhered soil: 1. Amount and particle-size distribution. Integr Environ Assess Manag 2:375–384. https://doi.org/10.1002/ieam.5630020409
151. Fabian MP, Miller SL, Reponen T, Hernandez MT (2005) Ambient bioaerosol indices for indoor air quality assessments of flood reclamation. J Aerosol Sci 36:763–783. https://doi.org/10.1016/j.jaerosci.2004.11.018
152. Da Silva LID, Yokoyama L, Maia LB, Monteiro MIC, Pontes FVM, Carneiro MC, Neto AA (2015) Evaluation of bioaccessible heavy metal fractions in PM10 from the metropolitan region of Rio de Janeiro city, Brazil, using a simulated lung fluid. Microchem J 118:266–271. https://doi.org/10.1016/j.microc.2014.08.004
153. Frey-Wehrmann S (1991) Bindungsformen von Blei, Zink, Cadmium und Kupfer in Böden der nördlichen Eifel, Aachen
154. Sundaray SK, Nayak BB, Lin S, Bhatta D (2011) Geochemical speciation and risk assessment of heavy metals in the river estuarine sediments—a case study: Mahanadi basin, India. J Hazard Mater 186:1837–1846. https://doi.org/10.1016/j.jhazmat.2010.12.081
155. Fekete A, Sandholz S (2021) Here comes the flood, but not failure? Lessons to learn after the heavy rain and pluvial floods in Germany 2021. Water 13:3016. https://doi.org/10.3390/w13213016
156. Bosseler B, Salomon M, Schlüter M, Rubinato M (2021) Living with urban flooding: a continuous learning process for local municipalities and lessons learnt from the 2021 events in Germany. Water 13:2769. https://doi.org/10.3390/w13192769
157. Thieken AH, Bubeck P, Heidenreich A, Keyserlingk J von, Dillenardt L, Otto A (2022) Performance of the flood warning system in Germany in July 2021—insights from affected residents. EGUsphere. https://doi.org/10.5194/egusphere-2022-244. **(preprint)**
158. Amato F, Querol X, Johansson C, Nagl C, Alastuey A (2010) A review on the effectiveness of street sweeping, washing and dust suppressants as urban PM control methods. Sci Total Environ 408:3070–3084. https://doi.org/10.1016/j.scitotenv.2010.04.025
159. Gozzard E, Mayes WM, Potter HAB, Jarvis AP (2011) Seasonal and spatial variation of diffuse (non-point) source zinc pollution in a historically metal mined river catchment, UK. Environ Pollut 159:3113–3122. https://doi.org/10.1016/j.envpol.2011.02.010

Publisher's Note